

ผลของการลดทอนปริมาณรังสีจากเตียงรังสีรักษาในเทคนิคการฉายรังสีแบบพิเศษ

นางสาวนฤมล เงินเดือน

วิทยานิพนธ์นี้เป็นส่วนหนึ่งของการศึกษาตามหลักสูตรปริญญาวิทยาศาสตรมหาบัณฑิต

สาขาวิชาอายุเวชศาสตร์ ภาควิชารังสีวิทยา

คณะแพทยศาสตร์ จุฬาลงกรณ์มหาวิทยาลัย

ปีการศึกษา 2555

ลิขสิทธิ์ของจุฬาลงกรณ์มหาวิทยาลัย

บทคัดย่อและแฟ้มข้อมูลฉบับเต็มของวิทยานิพนธ์ตั้งแต่ปีการศึกษา 2554 ที่ให้บริการในคลังปัญญาจุฬาฯ (CUIR)

เป็นแฟ้มข้อมูลของนิสิตเจ้าของวิทยานิพนธ์ที่ส่งผ่านทางบัณฑิตวิทยาลัย

The abstract and full text of theses from the academic year 2011 in Chulalongkorn University Intellectual Repository (CUIR)

are the thesis authors' files submitted through the Graduate School.

**THE ATTENUATION EFFECT OF TREATMENT COUCH IN ADVANCE RADIOTHERPY  
TECHNIQUES**

**Miss Narumol Nguanthean**

**A Thesis Submitted in Partial Fulfillment of the Requirements  
for the Degree of Master of Science Program in Medical Imaging**

**Department of Radiology**

**Faculty of Medicine**

**Chulalongkorn University**

**Academic Year 2012**

**Copyright of Chulalongkorn University**

นฤมล เงินเดือน: ผลของการลดทอนปริมาณรังสีจากเตียงรังสีรักษาในเทคนิคการฉายรังสีแบบพิเศษ.  
(THE ATTENUATION EFFECT OF TREATMENT COUCH IN ADVANCE  
TECHNIQUES) อ.ที่ปริกษาวิทยานิพนธ์หลัก: รศ.ศิวลี สุริยาปี, 65 หน้า.

จุดประสงค์ของการศึกษานี้คือ ศึกษาค่าตัวแปรที่มีผลต่อปริมาณรังสีเมื่อลำรังสีผ่านเตียงชนิด Exact และ Exact IGRT และเพื่อศึกษาผลของการลดทอนปริมาณรังสีเมื่อผ่านเตียงในเทคนิคการฉายรังสีแบบ 2 มิติ เทคนิคการฉายรังสีแบบปรับความเข้มและเทคนิคการฉายรังสีแบบปรับความเข้มรอบตัวผู้ป่วย ซึ่งจะใช้เครื่องเร่งอนุภาค 21 EX ที่ใช้เตียง Exact และเครื่องเร่งอนุภาค iX ที่ใช้เตียง Exact IGRT ในการทดลองนี้วัดด้วยลำโฟตอน 6 และ 10 MV ที่มีขนาดลำรังสี 3x3 ซม. 5x5 ซม. 10x10 ซม. และ 20x20 ซม. ในตำแหน่งต่างๆ ของเตียงคือ หัวเตียง กลางเตียง และปลายเตียง ผลการศึกษาตัวแปรพบว่ามีการลดทอนปริมาณรังสีสูงสุดที่ขนาดของลำรังสีแคบสุด คือ 3x3 ซม. ในทุกตำแหน่งของเตียง เมื่อลำรังสีผ่านเตียง Exact ในลักษณะของขอบเตียงเลื่อนเข้าที่ตำแหน่งหัวเตียง สำหรับ 6 MV ค่าลดทอนคือ 18.5% และ 10 MV คือ 14.7% ในตำแหน่งมุม 170 และ 190 องศา สำหรับเตียง Exact IGRT พบว่าการลดทอนปริมาณรังสีที่ผ่านเตียงสูงสุดบริเวณปลายเตียง สำหรับ 6 MV คือ 5.1% และ 10 MV คือ 5.0% ในตำแหน่งมุม 140 และ 220 องศา เมื่อพิจารณาแผนการรักษาในผู้ป่วย ปริมาณรังสีที่แตกต่างกันมากที่สุดระหว่างการวัดและการคำนวณแบบไม่มีเตียงพบที่แผนการรักษาทรงอกแบบ 2 ลำตรงข้ามกันของเตียง Exact ด้วยโฟตอน 6 MV คือ 7.69% และ 2.29% สำหรับการฉายทิศทางเดียวของการฉายกระดูกสันหลังของเตียง Exact IGRT ส่วนเปอร์เซ็นต์ความแตกต่างในเทคนิคการฉายรังสีแบบปรับความเข้มระหว่างวัดและการคำนวณโดยไม่มีเตียงมีค่าตั้งแต่ 2.67% ถึง 5.89% สำหรับเตียง Exact และ 0.67% ถึง 3.25% สำหรับเตียง Exact IGRT เปอร์เซ็นต์ความแตกต่างในเทคนิคการฉายรังสีแบบปรับความเข้มรอบตัวผู้ป่วยระหว่างวัดและการคำนวณโดยไม่มีเตียง มีค่าตั้งแต่ 2.87% ถึง 4.73% สำหรับเตียง Exact IGRT ความแตกต่างของปริมาณรังสีระหว่างการวัดและการคำนวณที่มีเตียงมีค่าน้อยกว่าความแตกต่างที่ไม่มีเตียงในทุกๆ เทคนิค สรุปได้ว่าผลจากการลดทอนปริมาณรังสีมีผลต่อการรักษาอย่างมีนัยสำคัญสำหรับผู้ป่วยที่ได้รับการรักษาด้วยการฉายรังสีด้านหลังและที่ทำมุมเอียงจากด้านหลัง การลดทอนปริมาณรังสีจะขึ้นอยู่กับ ขนาดของลำรังสี มุมที่ฉายรังสี พลังงาน ตำแหน่งของเตียง และชนิดของเตียงเพราะฉะนั้นการฉายรังสีผู้ป่วยควรหลีกเลี่ยงจากมุมที่ลำรังสีผ่านโดยตรงกับขอบเตียงด้านหลังและด้านเฉียง หรือเวลาที่วางแผนการรักษาควรจะได้เตียงรวมอยู่ในระบบ การวางแผนการรักษาด้วย

ภาควิชา..... รังสีวิทยา.....ลายมือชื่อนิสิต.....

สาขาวิชา.....ฉายาเวชศาสตร์..... ลายมือชื่อ อ.ที่ปริกษาวิทยานิพนธ์หลัก.....

ปีการศึกษา .....2555.....

##5474192830: MAJOR MEDICAL IMAGING

KEYWORDS: COUCH ATTENUATION/ EXACT COUCH/ EXACT IGRT  
COUCH/ IMRT/ VMAT

NARUMOL NGUANTHEAN: THE ATTENUATION OF TREATMENT  
COUCH IN ADVANCE RADIOTHERAPY TECHNIQUES. ADVISOR:  
ASSOC. PROF. SIVALEE SURIYAPEE, 65pp.

The purpose of this work is to study the dosimetric parameters influenced in Exact couch and the Exact IGRT couch attenuation and to determine the effect in conventional, IMRT and VMAT treatment techniques. The dose measurements were employed in both energies of 6 MV and 10 MV photon beams with field sizes of  $3 \times 3$  cm<sup>2</sup>,  $5 \times 5$  cm<sup>2</sup>,  $10 \times 10$  cm<sup>2</sup>, and  $20 \times 20$  cm<sup>2</sup> for various gantry angles around the treatment couch at cranial, middle and caudal couch position. The effect of couch attenuation in conventional, IMRT and VMAT treatment techniques were investigated. The maximum attenuation was detected at 6 MV with the smallest field for all couch positioning setups. The Exact couch showed maximum attenuation of 18.5% for 6 MV and 14.7% for 10 MV at 170 and 190 degree at rail in and cranial couch position, while the Exact IGRT couch presented the maximum attenuation of 5.1% for 6 MV and 5.0% for 10 MV at 140 and 220 degree at caudal position for  $3 \times 3$  cm<sup>2</sup> field size. The maximum percent dose differences between measurement and calculation without couch consideration for 6 MV in parallel opposing fields of chest treatment were 7.96% for Exact couch at rail in position and 2.29% from single field PA spine treatment for IGRT couch. The percent dose differences in IMRT plans between measurement and calculation without couch were varied from 2.67% to 5.89% for Exact couch and 0.67% to 3.25% for Exact IGRT couch. While VMAT plans presented the deviation from 2.87% to 4.73% for Exact IGRT couch. The percent dose differences between measurement and calculation with couch were smaller than without couch for all techniques study. The effect from beam attenuation by the treatment couch is significant for patients treated with posterior or oblique posterior fields. The dose deviation due to couch attenuation of Varian couch depends on the field size, angle beam, energy, couch position and type. Therefore, patients should be avoided from the beam pass directly through rail position in posterior and posterior oblique or the correction should be included in treatment planning systems.

Department: .....Radiology.....Student's Signature.....

Field of Study: ...Medical Imaging.....Advisor's Signature.....

Academic Year: .....2012.....

## ACKNOWLEDGEMENTS

I would like to deepest thank to Associate Professor Sivalee Suriyapee, M.Eng, Division of Therapeutic Radiology and Oncology, Department of Radiology, Faculty of Medicine, Chulalongkorn University, advisor, to advise, instruct and support for me, Mr. Taweap Sanghangtum, Ph.D., co advisor, for a very great suggestion for the improvement.

I would like to thank Mr. Sornjarod Oonsiri., Mrs. Puntawa Oonsiri., Mr. Isra Israngkul Na Ayuthaya., Miss Sumana Soomboon., Miss Chotoka Jampangern., and all staff in Division of Therapeutic Radiology and Oncology, Department of Radiology, Faculty of Medicine, King Chulalongkorn Memorial Hospital for a very kindness advice.

I would like to thank Associate Professor Anchali Krisanachinda, Ph.D., Division of Nuclear Medicine, Department of Radiology, Faculty of Medicine, Chulalongkorn University and all lecturers and staff in the Master of Science Program in Medical Imaging, Faculty of Medicine, Chulalongkorn University for their teaching of knowledge in Medical Imaging.

I would like to thank Professor Franco Milano, Ph.D., who was the external examiner of the thesis defense for his help, kind suggestion and comments in this research.

Finally, I would like to thank my family for a very great encouragement.

# CONTENTS

	<b>Page</b>
ABSTRACT (THAI).....	iv
ABSTRACT (ENGLISH).....	v
ACKNOWLEDGEMENTS.....	vi
CONTENTS.....	vii
LIST OF TABLES.....	x
LIST OF FIGURES.....	xii
LIST OF ABBREVIATIONS.....	xiv
<b>CHAPTER I INTRODUCTION</b>	
1.1 Background and Rationale.....	1
1.2 Research Objective.....	3
<b>CHAPTER II REVIEW OF RELATED LITERATURES</b>	
2.1 Theories.....	4
2.1.1 Basic of photon radiotherapy.....	4
2.1.2 Apparent linear absorption coefficient.....	5
2.1.3 Treatment planning.....	7
2.1.4 Treatment couch.....	9
2.1.5 Gamma evaluation.....	12
2.2 Review of Related Literature.....	15
<b>CHAPTER III RESEARCH METHODOLOGY</b>	
3.1 Research Design.....	18
3.2 Research Design Model.....	18
3.3 Conceptual Framework.....	19
3.4 Key Words.....	19
3.5 Research Questions.....	19
3.6 Materials.....	20
3.6.1 Varian Clinac 21EX linear accelerator.....	20
3.6.2 Varian Clinac iX linear accelerator.....	20
3.6.3 Ionization chambers.....	21
3.6.4 Electrometer.....	22

	<b>Page</b>
3.6.5 Eclipse treatment planning software.....	23
3.6.7 Three-dimensional diode arrays: ArcCHECK.....	23
3.6.8 Solid water phantom.....	24
3.6.9 IMRT/VMAT QA software.....	24
3.7 Methods.....	25
3.7.1 Basic parameters influenced the couches.....	25
3.7.2 Clinical application .....	28
3.8 Outcome Measurement .....	30
3.9 Data Collection.....	30
3.10 Data Analysis .....	31
3.11 Benefit of the Study.....	31
3.12 Ethical Consideration.....	31
 <b>CHAPTER IV RESULTS</b>	
4.1 Gravitation Effect of Gantry Rotation.....	32
4.2 Basic Parameters influenced the Exact Couch.....	34
4.2.1 Sliding rail out: cranial position.....	34
4.2.2 Sliding rail in: cranial position.....	37
4.2.3 Sliding rail out: caudal position.....	40
4.2.4 Sliding rail in: caudal position.....	43
4.2.5 Summary of field size effect for the Exact couch.....	46
4.3 Basic Parameters influenced the Exact IGRT Couch .....	47
4.3.1 Cranial position.....	47
4.3.2 Middle position.....	49
4.3.3 Caudal position.....	51
4.3.4 Summary of field size effect for the Exact IGRT couch...	52
4.4 Clinical Application .....	53
4.4.1 Conventional technique.....	53
4.4.2 Intensity-modulated radiation therapy (IMRT).....	55
4.4.3 Volumetric-modulated arc therapy (VMAT).....	57

	<b>Page</b>
<b>CHAPTER V DISCUSSION AND CONCLUSION</b>	
5.1 Discussion.....	58
5.1.1 Gravitation effect of gantry Rotation.....	58
5.1.2 Basic parameters influence the Exact couch.....	58
5.1.3 Basic parameters influence the Exact IGRT couch.....	59
5.1.4 Clinical application.....	60
5.2 Conclusions.....	61
5.3 Recommendation.....	62
<b>REFERENCES</b> .....	63
<b>VITAE</b> .....	65

.



## LIST OF TABLES

<b>Table</b>		<b>Page</b>
4.1	Gravitation effect of gantry rotation at various angles for 6 MV and 10x10 cm <sup>2</sup> field size.....	32
4.2	Gravitation effect of gantry rotation at various angles for 10 MV and 10x10 cm <sup>2</sup> field size.....	33
4.3	Relative doses from Exact couch for 6 MV with sliding rail out at cranial position for 3x3, 5x5, 10x10, and 20x20 cm <sup>2</sup> field sizes.....	35
4.4	Relative doses from Exact couch for 10 MV with sliding rail out at cranial position for 3x3, 5x5, 10x10, and 20x20 cm <sup>2</sup> field sizes.....	36
4.5	Relative doses from Exact couch for 6 MV with sliding rail in at cranial position for 3x3, 5x5, 10x10, and 20x20 cm <sup>2</sup> field sizes .....	38
4.6	Relative doses from Exact couch for 10 MV with sliding rail in at cranial position for 3x3, 5x5, 10x10, and 20x20 cm <sup>2</sup> field sizes.....	39
4.7	Relative doses from Exact couch for 6 MV with sliding rail out at caudal position for 3x3, 5x5, 10x10, and 20x20 cm <sup>2</sup> field sizes .....	41
4.8	Relative doses from Exact couch for 10 MV with sliding rail out at caudal position for 3x3, 5x5, 10x10, and 20x20 cm <sup>2</sup> field sizes .....	42
4.9	Relative doses from Exact couch for 6 MV with sliding rail in at caudal position for 3x3, 5x5, 10x10, and 20x20 cm <sup>2</sup> field sizes.....	44
4.10	Relative doses from Exact couch for 10 MV with sliding rail in at caudal position for 3x3, 5x5, 10x10, and 20x20 cm <sup>2</sup> field sizes .....	45
4.11	Maximum attenuation introduced by couch (with sliding rails out and in at cranial position for the Exact couch).....	47
4.12	Maximum attenuation introduced by couch (with sliding rails out and in at caudal position for the Exact couch).....	47
4.13	Relative doses from Exact IGRT couch for 6 MV at cranial position for 3x3, 5x5, 10x10, and 20x20 cm <sup>2</sup> field sizes .....	48

<b>Table</b>	<b>Page</b>
4.14	Relative doses from Exact IGRT couch for 10 MV at cranial position for 3x3, 5x5, 10x10, and 20x20 cm <sup>2</sup> field sizes ..... 48
4.15	Relative doses from Exact IGRT couch for 6 MV at middle position for 3x3, 5x5, 10x10, and 20x20 cm <sup>2</sup> field sizes ..... 49
4.16	Relative doses from Exact IGRT couch for 10 MV at middle position for 3x3, 5x5, 10x10, and 20x20 cm <sup>2</sup> field sizes ..... 50
4.17	Relative doses of Exact IGRT couch of 6 MV at caudal position for 3x3, 5x5, 10x10, and 20x20 cm <sup>2</sup> field sizes..... 51
4.18	Relative doses of Exact IGRT couch of 10 MV at caudal position for 3x3, 5x5, 10x10, and 20x20 cm <sup>2</sup> field sizes..... 51
4.19	The maximum attenuation introduced by couch at cranial, middle and caudal position for the Exact IGRT couch..... 53
4.20	Dose difference between calculation and measurement with the sliding rail “out” position of conventional techniques for the Exact couch ..... 54
4.21	Dose difference between calculation and measurement with the sliding rail “in” position of conventional techniques for the Exact couch ..... 54
4.22	Dose difference between measurement with and without couch of conventional technique for the Exact IGRT couch..... 55
4.23	The percent gamma pass and percent dose difference between measurements compared to planning with and without couch insertion for IMRT techniques at the Exact couch..... 56
4.24	The percent gamma pass and percent dose difference between measurements compared to planning with and without couch insertion for IMRT technique at the Exact IGRT couch..... 56
4.25	The percent gamma pass and percent dose difference between measurement compared to planning with and without couch insertion of the VMAT technique for the Exact IGRT couch..... 57

## LIST OF FIGURES

Figure		Page
1.1	The Exact couch and the Exact IGRT couch.....	3
2.1	Schematic of a linear accelerator.....	4
2.2	Diagram illustrating how the absorber of thickness $\Delta x$ reduces the intensity of radiation at P, and how scattered radiation is produced...	6
2.3	Treatments planning of IMRT.....	8
2.4	Treatment planning of VMAT.....	9
2.5	Structure of the couch: a) the Exact IGRT couch and b) the Exact couch.....	12
2.6	Schematic representation of the theoretical concept of the gamma evaluation method.....	14
3.1	Research design model.....	18
3.2	Conceptual frameworks.....	19
3.3	Varrian Clinac 21 EX .....	20
3.4	Varian Clinac iX.....	21
3.5	The ionization chamber: a) FC65-P and b) CC13.....	22
3.6	The DOSE-1 dosimeter.....	22
3.7	Eclipse treatment planning: version 8.9.17.....	23
3.8	Three-dimensional diode arrays: ArcCHECK <sup>TM</sup> .....	24
3.9	Solid water phantoms.....	24
3.10	SNC Patient software.....	25
3.11	The chamber with buildup setting up on Varian Clinac iX linear accelerator.....	26
3.12	The Exact couch: a) sliding rail out and b) sliding rail in position.....	26
3.13	The chamber and phantom setting up on Exact couch and diagram of gantry angle.....	27
3.14	The chamber and phantom setting up on Exact IGRT couch.....	28
3.15	Dose distributions of a) IMRT and b) VMAT techniques.....	30

<b>Figure</b>	<b>Page</b>
4.1 The polar plot of relative dose for gravitation effect of gantry for 10x10 cm <sup>2</sup> field size: a) 6 MV and b) 10 MV.....	34
4.2 The polar plot of relative dose for Exact couch with rail out position for 3x3, 5x5, 10x10, and 20x20 cm <sup>2</sup> field sizes: a) 6 MV and b) 10 MV.....	37
4.3 The polar plot of relative dose for Exact couch with rail in position for 3x3, 5x5, 10x10, and 20x20 cm <sup>2</sup> field sizes: a) 6 MV and b) 10 MV.....	40
4.4 The polar plot of relative dose for Exact couch with rail out position for 3x3, 5x5, 10x10, and 20x20 cm <sup>2</sup> field sizes: a) 6 MV and b) 10 MV.....	43
4.5 The polar plot of relative dose for Exact couch with rail in position for 3x3, 5x5, 10x10, and 20x20 cm <sup>2</sup> field sizes: a) 6 MV and b) 10 MV.....	46
4.6 The polar plot of relative dose at cranial position for the Exact IGRT couch for 3x3, 5x5, 10x10, and 20x20 cm <sup>2</sup> field sizes: a) 6 MV and b) 10 MV.....	49
4.7 The polar plot of relative dose at middle position for the Exact IGRT couch for 3x3, 5x5, 10x10, and 20x20 cm <sup>2</sup> field sizes: a) 6 MV and b) 10 MV.....	50
4.8 The polar plot of relative dose at caudal position for the Exact IGRT couch for 3x3, 5x5, 10x10, and 20x20 cm <sup>2</sup> field sizes: a) 6 MV and b) 10 MV.....	52

## LIST OF ABBREVIATIONS

ABBREVIATION	TERMS
2D	Two-Dimensional
3D	Three-Dimensional
AAA	Analytical Anisotropic Algorithm
cGy	Centigray
cm	Centimeter
ICRU	International Commission on Radiation Units and Measurement
IMRT	Intensity Modulated Radiotherapy
LINAC	Linear Accelerator
MV	Megavoltage
MeV	Mega Electron Volt
mm	Millimeter
MU	Monitor Unit
QA	Quality Assurance
VMAT	Volumetric Modulated Arc Therapy
CT	Computed Tomography
TPS	Treatment Planning System
EPID	Electronic Portal Imaging Device
CBCT	Cone Beam Computed Tomography
IAEA	International Atomic Energy Agency
IC	Ionization Chamber
IGRT	Image Guided Radiation Therapy
HVL	Half-Value Layer
MLC	Multileaf Collimator
SSD	Source to Surface Distance
SAD	Source to Axis Distance
MBS	Model-Based Segmentation

PMMA	Polymethyl methacrylate
POM	PolyOxyMethylene
AP	Anteroposterior
PA	Posteroanterior
SD	Standard Deviation
IEC	International Electrotechnical Commission
ADCLs	Advanced Data Collection Location System
TNC	Threaded Neill–Concelman
BNC	Bayonet Neill–Concelman

# CHAPTER I

## INTRODUCTION

### 1.1 Background and Rationale

Nowadays, the mortality of cancer patient is increasing rapidly and the death rate from cancer is in the top rank in worldwide. Radiotherapy is one of the main cancer treatment methods that used high radiation dose. The treatment techniques has been developed from conventional to advance technique in order to conform the high radiation dose to cancer target and spare the radiation dose to surrounding normal tissues [1]. Modern radiotherapy relies on accurate dose delivery to the prescribed target volume. The International Commission on Radiation Units and Measurement (ICRU) recommended an overall accuracy in tumor dose delivery of  $\pm 5\%$ , based on an analysis of dose response data and on an evaluation of errors in dose delivery in a clinical setting. Considering all uncertainties involved in the dose delivery to the patient, the  $\pm 5\%$  accuracy recommendation is by no means easy to attain [2].

In radiotherapy, radiation treatment planning is the process in which a team consisting of radiation oncologists, radiation therapists, medical physicists and medical dosimetists plan the appropriate radiotherapy technique for a cancer patient. Patient anatomy and tumour targets can be represented as 3-D models. The entire process of treatment planning involves many steps and the medical physicist is responsible for the overall integrity of the computerized treatment planning (TPS) to accurately and reliably produce dose distribution and associated calculations for external beam radiotherapy. In present, the treatment techniques are used such as conventional, Intensity Modulated Radiotherapy (IMRT) and Volumetric Modulated Arc Therapy (VMAT). The improvement in malignancy-detection has also led to an improvement in the ability to treat disease with an increasing ability to spare surrounding normal tissues and structures [3].

The most cancer patient population receiving from radiation therapy, there is a need for continual research and investigation into methods for ensuring adequate and accurate radiation dose to treatment volumes and dose-sparing to critical structures. The attenuation of treatment couches for patient positioning is one of the works that

needed to be studied. There is an assumption that the treatment couch is a radio-translucent. So it is not generally taken into account during treatment planning. The patients are positioned prone or supine on a treatment couch for radiation therapy. The patient couch is meant to provide a means for reproducible patient positioning. Patients can be further positioned with the use of various devices such as masks to hold the head and neck in a fixed position or cradles that hold the body in fixed position, but these are patient-specific and treatment-specific devices that are separated from the treatment couch. Given the necessity for the couch to be rigid enough to support large patients without sagging, the construction material of the treatment couch has two important constraints: it must be strong and durable enough to meet manufacturer's sag tolerances and it should be radio-transparent enough to not appreciably attenuate the therapy beam when radiation fields intersect the couch. The couch tops are generally made of carbon fiber, which has a low density, and therefore considered to be radio-translucent. In some model, the couch is supported by carbon fiber rails that allow the couch to move forward and backward for correction of patient positioning and can also be moved laterally in and out. However, many studies in investigating beam attenuation by treatment couches and rails have shown relatively large amounts of beam attenuation at angles over which the beam transverses the couch and rails.

The optimized parameters, such as beam energy, field size, depth, technique, angle beam, wedge, and types of couch are put into the treatment planning to calculate the radiation dose distribution. The posterior and posterior oblique treatment fields are routinely used in the treatment of various diseases, however, the couch attenuation effects are not considered in the traditional planning software versions. The new planning software can add couch in the program.

The problem inferred by the attenuations observed in these studies is the potential effect on patient with posterior and posterior oblique fields. Since the treatment couch is not normally accounted in the treatment planning, the dosimetric effect of the attenuation on target and normal tissue structures cannot be anticipated. The result would be caused clinically unacceptable losses of dose and coverage to the target structures associated with head, chest and pelvis cancer treatment.



In this study, two types of Varian couches (Varian Medical Systems, Palo Alto, CA); the Exact couch and the Exact IGRT couch are used to investigate the attenuate effect. Both couches are shown in figure 1.1.



(a)

(b)

**Figure 1.1** a) The Exact couch and b) the Exact IGRT couch

The aim of this work is to determine the parameters affected the dose attenuated in passing two types of couches and to measure the beam attenuation for various treatment techniques of conventional, IMRT and VMAT. The measurements are compared with the treatment planning calculation for both with and without couch insertion.

## 1.2 Research Objectives

1. To study the dosimetric parameters influenced on the Exact couch and the Exact IGRT couch attenuation.
2. To determine the dose effect of couch attenuation for conventional, IMRT, and VMAT treatment techniques with and without couch insertion.

## CHAPTER II

### LITERATURE REVIEWS

#### 2.1 Theories

##### 2.1.1 Basics of photon radiotherapy [1]

External photon beam therapy utilizes a linear accelerator to produce a beam of high energy that can be used for patient exposure. A linear accelerator produces the x-ray beam by first producing a beam of high-energy electrons and aiming the electron beam at a target made of material with a high atomic number. The interactions of these electrons with the target result in Bremsstrahlung x-ray emissions that form a resultant treatment x-ray beam. This x-ray beam is shaped first by a primary set of collimators, found directly behind the x-ray target. Because the x-ray beam is heterogeneous, a flattening filter is used to influence the energy uniformity of the beam before it passes through a second set of moveable collimators. The primary collimators are stationary, but the secondary collimators are made of lead or tungsten piece, which allow for treatment field size variation through adjustment of each piece.

Linear accelerators used for isocentric treatments have a gantry that allows for a full 360° rotation around the system's isocenter, the point where the axis of rotation of the secondary collimator perpendicularly intersects the gantry's rotational axis. It is shown in figure 2.1. This rotation allows the treatment beam to enter the target medium at a designated angle of incidence.

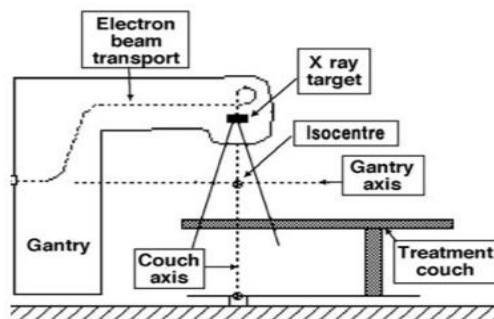


**Figure 2.1** Schematic of a linear accelerator [1].

### 2.1.2 Apparent linear absorption coefficient [4]

When an x-ray beam passes into an absorbing medium, such as carbon fiber, x-ray photons may interact with the absorber to produce high speed electrons by three distinct mechanisms known as the photoelectric process, the Compton process and pair-production process take place simultaneously. Suppose a device which can record the number of photons that pass through it is placed in an x-ray beam at point P in figure 2.2. Let the number of photons recorded be N. If a slab of material thickness  $\Delta x$  is placed in the path of the x-rays, a number,  $\Delta N$ , of the photons will be removed from the beam and the number reaching P will be reduced. A photon cannot be partially stopped by the atoms in the slab of material. It will either come close enough to the atom to interact and thus be removed from the beam or it will not be affected at all. Hence the number,  $\Delta N$ , which are removed, will depend directly on the number of photons present. If N is doubled, then the chances of an interaction will be doubled.  $\Delta N$  will also depend directly on the thickness of  $\Delta x$ . If  $\Delta x$  is doubled the number of atoms placed in the beam is doubled and so the chance of interaction is doubled. Mathematically, we may say that  $\Delta N$  varies as the product of N and  $\Delta x$ . Symbolically this can be written

$$\Delta N = -\mu N \Delta x \quad (2.1)$$

where  $\mu$ , the constant of proportionality, is called the linear absorption coefficient, or more correctly the apparent linear absorption coefficient,  $\mu$  depends on a complicated way on the atomic number Z of the absorbing material and the energy E of the radiation but for given values of Z and E, it has a definite value. It should be considered as a constant. The negative sign is necessary because as  $\Delta x$  increases, the number of photons in the beam decreases. Equation (2.1) may be rearranged as follows:

$$\mu = \frac{-\Delta N}{N} \times \frac{1}{\Delta x} \quad (2.2)$$

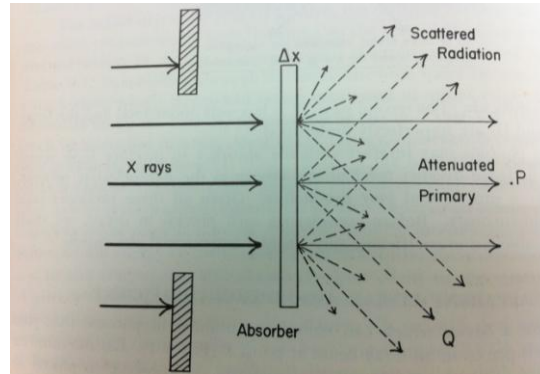


**Figure 2.2** Diagram illustrating how the absorber of thickness  $\Delta x$  reduces the intensity of radiation at P, and how scattered radiation is produced.

Since  $\Delta N/N$  is the ratio of two numbers and  $\Delta x$  is a thickness,  $\mu$  must have a dimension of 1 divided by a thickness. If  $x$  is measured in centimeter, the  $\mu$  will be measured in  $1/\text{cm}$  or  $\text{cm}^{-1}$ . To illustrate the meaning of  $\mu$ , let us suppose it has the value  $0.01 \text{ cm}^{-1}$  and that we are dealing with a 1 cm thickness of absorber. From (2.1) we see that  $\Delta N = -0.01 N$  which means that 1% of the photons are removed from the beam in a layer 1 cm thick. The linear absorption coefficient is therefore numerically equal to the fractional number of photons removed from the beam per cm of absorber. Since the number of photons which pass through a square cm per second determines the intensity  $I$  of the beam of radiation, equation (2.2) can equally well be written

$$\Delta I = -\mu I \Delta x \quad (2.3)$$

where  $I$ , the intensity, is proportional to  $N$  of equation (1), and  $\Delta I$ , the change in intensity, is proportional to  $\Delta N$  the number of photons removed from the beam.  $\Delta I$  thus gives the change in intensity of the beam produced by the absorber of thickness  $\Delta x$ . By an argument similar to the one above, it follows that the linear absorption coefficient is equal to the fractional reduction in intensity produced by 1 cm of absorber.

### 2.1.3 Treatment planning [5]

Radiation treatment planning requires the calculation of a set of parameter for the delivery of a certain radiation dose to the patient. Ideally, radiation dose distribution should be designed to conform perfectly to the entire tumor volume while completely avoiding surrounding normal tissues. Although achievement of this goal is practically impossible, a computer optimization can potentially simplify the tedious planning procedure and yield best possible plans. Computer optimization becomes necessary for conventional, IMRT and VMAT treatment planning system.

#### 2.1.3.1 Conventional technique [6]

Conventional technique mainly consists of a beam of radiation delivered to the patient from several directions: often front or back (uses single field), and both sides (two-parallel opposing fields). Conventional refers to the way the treatment is planned or simulated on a specially calibrated diagnostic x-ray machine known as a simulator because it recreates the linear accelerator actions, and to the usually well-established arrangements of the radiation beams to achieve a desired plan.

#### 2.1.3.2 Intensity modulated radiation therapy [7]

IMRT is an advanced mode of high precision radiotherapy that utilizes computer-controlled linear accelerators to deliver precise radiation doses to a malignant tumor or specific areas within the tumor. IMRT allows for the radiation dose to conform more precisely to the three dimensional shape of the tumor by modulating or controlling the intensity of the radiation beam in multiple small volumes. IMRT also allows higher radiation doses to be focused to regions within the tumor while minimizing the dose to surrounding normal critical structures. Treatment is carefully planned by using 3D computed tomography (CT) or magnetic resonance (MRI) images of the patient in conjunction with computerized dose calculations to determine the dose intensity pattern that will best conform to the tumor shape. Typically, combinations of multiple intensity-modulated fields coming from different beam directions produce a custom tailored radiation dose that maximizes tumor dose while also minimizing the dose to adjacent normal tissues. The treatment plan of IMRT is shown in figure 2.3.

Because the ratio of normal tissue dose to tumor dose is reduced to a minimum with the IMRT approach, higher and more effective radiation doses can safely be delivered to tumors with fewer side effects compared with conventional radiotherapy techniques. IMRT also has the potential to reduce treatment toxicity, even when doses are not increased. Due to its complexity, IMRT does require slightly longer daily treatment times and additional planning and safety checks before the patient can start the treatment.

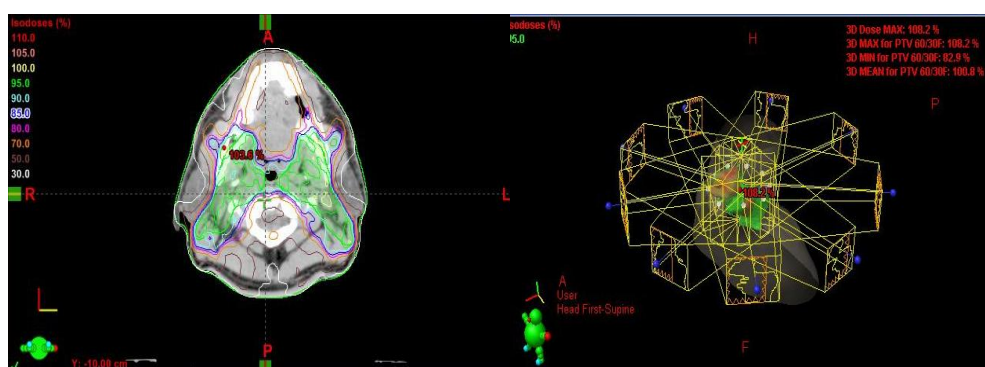


**Figure 2.3** Treatments planning of IMRT

### 2.1.3.3 Volumetric modulated radiotherapy [8]

VMAT delivers radiation by rotating the gantry of a LINAC through one or more arcs with the radiation continuously on. As it does so, a number of parameters can be varied. These include: MLC aperture shape, the fluence output rate, the gantry rotation speed and the MLC orientation. It is undisputed that VMAT can deliver highly conformal dose distributions similar to those created by other forms of IMRT. As such, it becomes a valued member of the IMRT delivery arsenal. The treatment plan of VMAT is shown in figure 2.4. VMAT most operate by creating some form of fixed-field modulated beams, decomposing these into MLC components, redistributing those over small arcs and re-optimizing the outcome. In doing so, VMAT can take advantage of the above mentioned four variable parameters, but must do so while respecting the physical constraints of the LINAC and MLC such as the maximum gantry speed, maximum leaf speed, the MLC orientation constraints and the available subdivisions of fluence output rate.

Provided that the gantry speed can be varied continuously, it does not require a continuous variation of fluence output rate to obtain a continuous variability of fluence output rate per degree. The minimum fluence output rate and the maximum gantry speed determine the constraining minimum fluence output rate per degree. Where there is a maximum fluence output rate and minimum gantry speed, there will be a constraining maximum fluence output rate per degree. VMAT can generate equivalently conformal dose distributions with fewer MU in a faster time. To have that is clearly advantageous these include: shorter treatments; better for patients in discomfort; less susceptibility to intra-fraction motion; possibly less induced secondary cancers; quicker overall treatment slots.

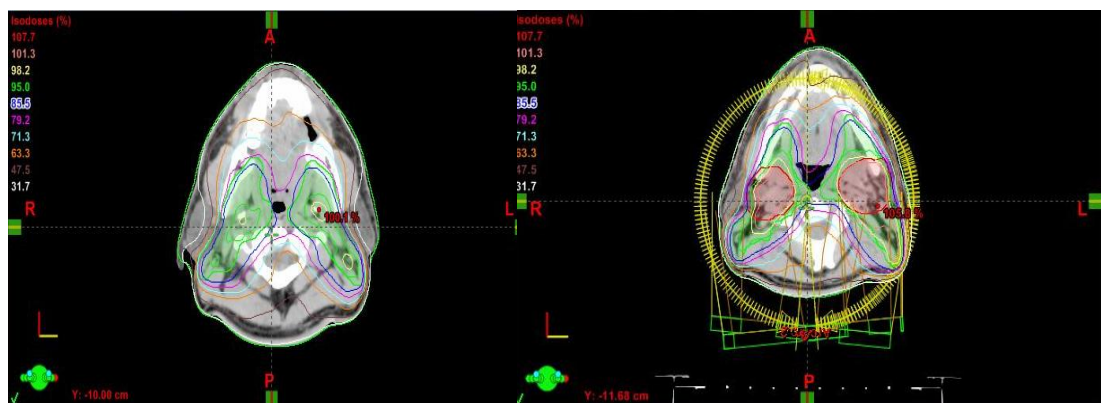


**Figure 2.4** Treatment planning of VMAT

### 2.1.4 Treatment couch [9]

Photon beam with a treatment couch depends on the same variables prevalent during the photon beam's interaction with skin tissue; field size, beam energy, source to surface distance, and beam angle. The penetration of the beam depends on the energy of the incident photons and the atomic number of the material being traversed influences the attenuation coefficient of the absorbing material. This is due to the idea that the attenuation coefficient represents the likelihood of the photon beam running into a particle which it will interact. Typical treatment couches installed on clinically used linear accelerators are composed of multiple layers. One of the most common combinations of couch materials is the use of carbon fiber layers around an inner

foam section. Carbon has an atomic number of 6, which reduces the probability of pair production and photoelectric absorption interactions occurring with megavoltage treatment photon beams. This reduces the amount of attenuation of the treatment beams before target medium interactions.

#### 2.1.4.1 Treatment machine and couch features [10]

Isocentrically mounted treatment machines rotate around an axis on which lies the isocentre. The isocentre is an important point in relation to the specification of dose. For routine treatment techniques the isocentre is required to be at a specified point in the patient. The design of the treatment couch and various ancillary devices influences the processes required to achieve the desired set-up. The light beam representing the radiation beam, and the cross representing the beam central axis or beam applicators are also used in the setting-up process.

#### 2.1.4.2 The treatment couch and its movements [10]

The couch is supported by a structure which allows both vertical and rotational movement. This may be a cylindrical ram which requires some depth of pit so that it can extend below floor level. Alternatively the support may be a pedestal structure, attached to a rotatable floor section. For flexibility in use, a couch rotation range well in excess of  $180^\circ$  is required. Some models are limited to  $\pm 90^\circ$  which restricts the usefulness of the treatment machine, being impractical for some types of set-up.

The range of vertical movements of the couch should be large, so that a low height is available to facilitate patient access, and for skin distance treatments. The ram type allows a lower minimum height and is less bulky, allowing more freedom for under-couch set-ups as well as complete tabletop removal and ram retraction to leave a clear floor area for special applications. Extra height should be available where long and for skin distance. Under - couch field, e.g. whole trunk, are to be used. Both systems may provide this if an appropriate model is chosen; however, the ram type, although allowing more height extension, requires a deep pit which is an expensive installation feature. The specified accuracy allows that a point on the



treatment couch may move up to 1 mm in any direction during a 10 cm vertical couch movement.

#### 2.1.4.3 Types of the couch

Two types of Varian couches (Varian Medical Systems, Palo, Alto, CA), the Exact couch and the Exact IGRT couch, are shown in figure 2.5. Structural of the Exact IGRT couch, is composed mostly of carbon fibers, and no metal components allowing for its use in imaging. Carbon fiber is a material consisting of fibers about 5–10  $\mu\text{m}$  in diameter and composed mostly of carbon. The carbon atoms are bonded together in crystals that are more or less aligned parallel to the long axis of the fiber. The properties of carbon fibers, such as high stiffness, high tensile strength, low weight, high chemical resistance, high temperature tolerance and low thermal expansion, make them very popular in couch of Varian. The Exact IGRT couch increases in thickness moving longitudinally from the section of the couch used for brain treatments, section of the couch used for chest towards the section used for abdomen treatments. Various thicknesses affect the attenuation of radiation to be different.

The Exact couch is different from the structure of the Exact IGRT couch. The carbon fiber in Exact couch is divided into two parts. The cranial position consists of carbon fiber with a thickness of 2.5 cm. the carbon fiber with a wide of 1.5 cm and at the net with a wide of 1.0 mm. For the caudal position consists of carbon fiber with a thickness of 1.9 cm carbon fiber with a length of 3.1 cm and two carbon sliding rails beneath the carbon plate for stabilization purposes with a height of 8.5 cm and 3.5 cm for width. The sliding rail for movement at” in” and “out” position and the sliding rail should not be positioned to cover the beam. In each section of the couch is the density of carbon as well.



**Figure 2.5** Structure of the couch: a) the Exact IGRT couch and b) the Exact couch

### 2.1.5 Gamma evaluation [11]

Regardless of the measurement technique, what is essential to the QA of the intensity modulated dose delivery is the efficient and accurate comparison of the measured versus calculated dose distribution. Van Dyk et al. [12] subdivided the dose distribution comparisons into regions of high and low dose gradients, each with a different acceptance criterion. In low gradient regions, the doses are compared directly with an acceptance tolerance placed on the difference between the measured and calculated doses. Visualization of the dose difference distribution identifies regions of disagreement. Because the dose difference in high dose gradient regions may be misleading, Van Dyk et al. used the concept of DTA. The DTA is the distance between a reference data point and the nearest point in the compared dose distribution that exhibits the same dose. The evaluation images displaying the dose difference and DTA are complementary in determining the acceptability of dose calculation versus delivery. In order to merge both evaluation images into a single image, a composite analysis used by Harms et al. uses a pass–fail criterion of both the dose difference and DTA: points that fail both criteria are identified on a composite distribution. The dose difference is displayed with the binary composite distribution highlighting regions of disagreement. A limitation of this technique is that the display of the dose difference may accentuate the impression of failure in high dose gradient regions. Also, it provides no quantitative measure of the magnitude of disagreement. The method presented by Low et al. [13] to simultaneously incorporate the dose and distance criteria. This method provides a numerical quality index referred to as the gamma

value that serves as a measure of disagreement in the regions that fail the acceptance criteria and indicates the calculation quality in regions that pass.

#### 2.1.5.1 Gamma evaluation theoretical concept

The gamma method is designed for the comparison of two dose distributions: one is defined to be the reference information  $D_r(r_r)$  and the other is queried for evaluation  $D_c(r_c)$ . A schematic representation of the gamma analysis tool for two dimensional dose distribution evaluations is shown in figure 2.6. The acceptance criteria are denoted by  $\Delta D_M$  for the dose difference and  $\Delta d_M$  for the distance to agreement. For a reference point at position  $r_r$ , receiving dose  $D_r$ , the surface representing these acceptance criteria are an ellipsoid defined by:

$$1 = \sqrt{\frac{\Delta r^2}{\Delta d_M^2} + \frac{\Delta D^2}{\Delta D_M^2}} \quad (2.4)$$

Where

$\Delta r = |r_r - r_c|$  is the distance between the reference and compared point and is the  $\Delta D = D_c(r_c) - D_r(r_r)$  dose difference at the position  $r_c$  relative to the reference dose  $D_r$  in  $r_r$ . For the compared distribution to match the reference dose in  $r_r$ , it need to contain at least one point  $(r_c, D_c)$  lying within the ellipsoid of acceptance, i.e. one point for which:

$$\gamma_r(r_c, D_c) = \sqrt{\frac{\Delta r^2}{\Delta d_M^2} + \frac{\Delta D^2}{\Delta D_M^2}} \leq 1 \quad (2.5)$$

A quantitative measure of the accuracy of the correspondence is determined by the point with the smallest deviation from the reference point, i.e. the point for which  $\gamma_r(r_c, D_c)$  is minimal. This minimal value is referred to as the quality index  $\gamma(r_r)$  of the reference point. The pass–fail criterion therefore becomes

$\gamma(r_r) \leq 1$ , correspondence is within the specified acceptance criteria,  
 $\gamma(r_r) > 1$ , correspondence is not within specified acceptance criteria.

An implicit assumption is made that once the passing criteria are selected, the dose difference and DTA analyses have equivalent significance when determining calculation quality.

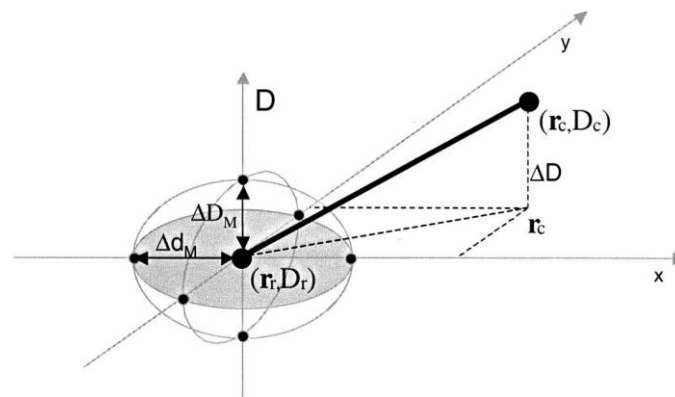


**Figure 2.6** Schematic representation of the theoretical concept of the gamma evaluation method

## 2.2 Review of Related Literature

**Li H, et al.** [14] studied the relationship of the dose for two Varian 21EX linear accelerators. The first machine was equipped with the standard couch with the sliding rail in and out position, while the secondary machine equipped with the exact IGRT carbon fiber couch. Measurements were performed using an ion chamber placed at the center of an acrylic cylindrical phantom positioned at the linac isocenter for 6 MV and 18 MV photon beams. The measurements were performed at field size of  $3 \times 3 \text{ cm}^2$ ,  $5 \times 5 \text{ cm}^2$  and  $10 \times 10 \text{ cm}^2$ , the maximum attenuation of 6 MV in Exact couch of the sliding rail in at pelvis position were 16.0%, 15.6% and 14.4%, respectively, and 3.8 to 4.8% at  $5 \times 5 \text{ cm}^2$  and 2.9 to 4.1% at  $10 \times 10 \text{ cm}^2$  for the exact IGRT couch. Evaluation of beam attenuation in two test IMRT plans and two tests VMAT plans, the standard couch attenuated the radiation beam up to 26.8%, while the carbon fiber IGRT couch attenuated the beam up to 4.1%. The highest dose difference between rails set at the “in” and “out” positions was 2.6% in the IMRT case and 2.1% in the VMAT case.

**Vieira SC, et al.** [15] studied individualized dosimetric quality assurance protocol for IMRT. This protocol includes dosimetric measurements with a fluoroscopic electronic portal imaging device (EPID) for all IMRT fields while the patient is being irradiated. For some of the patients enrolled in this protocol, significant beam attenuation by carbon fiber components of the treatment couch was observed. Studying the beam attenuation in two-dimensional, EPID images were also acquired in absence of the patient, both with and without treatment couches and immobilization devices, as positioned during treatment. If the couch table top is rotated to  $180^\circ$ , the beam attenuation is reduced to 5% because this part of the insert is hollow. For  $210^\circ$  gantry angle at the lung with immobilization device, 5% and 10% attenuation were observed for the support and for the pin used to attach the arm supported to the base plate, respectively. For treatments of head and neck cancer patients with a 6 MV photon beam, attenuation of up to 15% was detected. These

findings led to the development of new tools and procedures for planning and treatment delivery to avoid under dosages in the tumor.

**Seppälä JKH, et al.** [16] evaluated the interaction of 6 and 15 MV photons with eight different couch inserts. The presented results enable direct comparison of the attenuation properties of the studied couch tops. With a direct posterior beam, the maximum attenuations reach 3.6% and 2.4% with 6 and 15 MV, respectively. The measured maximum attenuation by a couch top with an oblique gantry angle was 10.8% and 7.4% at 6 and 15 MV energies, respectively. The skin-sparing effect was decreased substantially with every couch top. The highest increases in surface doses were recorded to be four- and threefold, as compared to the direct posterior open field surface doses of 6 and 15 MV, respectively. In conclusion, the carbon fiber tabletops decrease the skin-sparing effect of megavoltage photon energies. The increased beam attenuation and skin doses should be taken into account in the process of treatment planning.

**Hu Z, et al.** [17] evaluated beam attenuation of treatment couch and built a treatment couch model in TPS to check for beam–couch intersection at the planning stage and deal with beam attenuation by treatment couch in dose calculation. In this study, a standard treatment couch, Siemens ZXT couch, has been incorporated into Pinnacle 8.0 TPS, based on an existing TPS tool, model-based segmentation (MBS). This was done by generating the couch’s model from contours of the couch, together with the density information. Both the geometric and dosimetric accuracy of the couch model were evaluated. The test of beam–couch intersection prediction showed good agreement between predicted and measured results, and the differences were within 1 gantry rotation. For individual posterior oblique beams, the attenuation by metallic frames and PMMA couch top could reach nearly as high as 60% and 10%, respectively. For several posterior oblique beams ( $180^\circ$ ,  $220^\circ$ ,  $235^\circ$ ) that attenuated by the PMMA couch top, the calculated and measured dose distributions were compared. The dose differences at central axis were within 1%, and almost all points agreed with the calculations when the DD and DTA criteria of 3%/3 mm were adopted. The difference between calculated and measured attenuation factors were within 0.5%. This study demonstrates that the couch model created by MBS, which

contains geometric and density information of the couch, can be used to detect the beam–couch intersection, and also is able to provide an accurate representation of the couch top attenuation properties in patient dose calculation.

## CHAPTER III

### RESEARCH METHODOLOGY

#### 3.1 Research Design

This study is an observational descriptive study

#### 3.2 Research Design Model

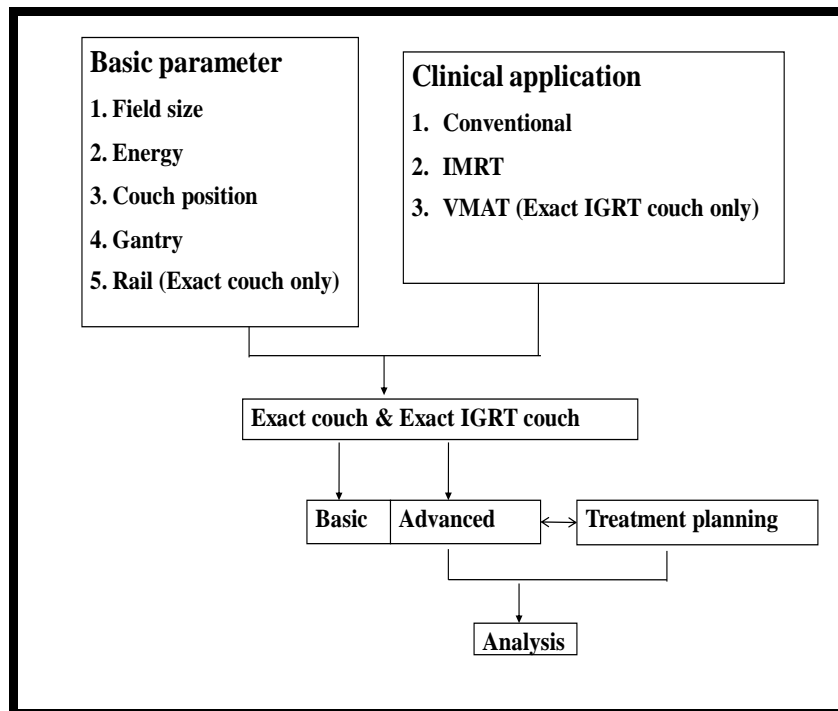


Figure 3.1 Research design model



### 3.3 Conceptual Framework

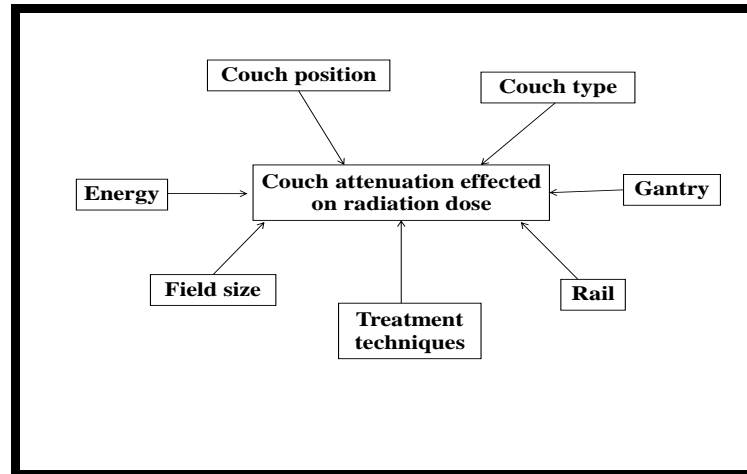


Figure 3.2 Conceptual frameworks

### 3.4 Key Words

- Couch attenuation
- Exact couch
- Exact IGRT couch
- Intensity Modulated Radiation Therapy (IMRT)
- Volumetric Modulated Arc Therapy (VMAT)

### 3.5 Research Questions

#### 1. Primary Research Question

What are the dosimetric parameters influenced on the Exact couch and the Exact IGRT couch attenuation?

#### 2. Secondary Research Question

What are the dose effects of couch attenuation for conventional, IMRT, and VMAT treatment techniques with and without couch?

### 3.6 Materials

#### 3.6.1 Varian Clinac 21EX linear accelerator

Varian Clinac 21EX linear accelerator (Varian Oncology Systems, Palo Alto, CA, USA) with 80 multileaf collimator operated in 6, 10 MV photon beams, and five electron beam energies of 6, 9, 12, 16, and 20 MeV. Photon field sizes are ranged from  $0.5 \times 0.5 \text{ cm}^2$  to  $40 \times 40 \text{ cm}^2$  at isocenter. The distance from the target to isocenter is 100 cm. The dose rates are ranged from 100-600 monitor units per minute. This machine is equipped with the Exact couch as shown in figure 3.3.



**Figure 3.3** Varian Clinac 21 EX

#### 3.6.2 Varian Clinac iX linear accelerator

Varian Clinac iX linear accelerator (Varian Oncology Systems, Palo Alto, CA, USA) with 120 multileaf collimator operated in 6, 10 MV x-ray, six electron beam energies of 4, 6, 9, 12, 16, and 20 MeV. Photon field sizes are ranged from  $0.5 \times 0.5 \text{ cm}^2$  to  $40 \times 40 \text{ cm}^2$  at isocenter. The distance from the target to isocenter is 100 cm. The dose rates are ranged from 100-600 monitor units per minute. This machine is equipped with the Exact IGRT couch as shown in figure 3.4.



**Figure 3.4** Varian Clinac iX

### **3.6.3 Ionization chambers [18]**

The  $0.65 \text{ cm}^3$  FC65-P is an ionization chamber (Wellhöfer Dosimetrie, Schwarzenbruck, Germany) of a classic Farmer design, intended for absolute dosimetry that meet or exceed performance standards of the original Farmer design. Similarities to the original Farmer include conformity to all external physical dimensions, a choice of thimble material sensitive volumes of  $0.65 \text{ cc}$  and atmospheric communication. Additional features are not shared with the original Farmer include guarding up to the measuring volume and waterproof construction. The FC65-P model is most closely resembles the NE 2581A, that it has a rugged thimble made of Delrin (POM, poly-oxymethylate), an aluminum center electrode. The FC65-P ionization chamber is shown in figure 3.5 (a).

The  $0.13 \text{ cm}^3$  CC13 ionization chamber (Wellhofer Dosimetrie, Schwarzenbruck Germany) can measure absolute and relative dosimetry of photon and electron beams in radiotherapy by planning in solid phantoms or in water phantoms. The sensitivity of CC13 is  $2.647 \times 10^8 \text{ Gy/C}$ . The CC13 ionization chamber is shown in figure 3.5 (b).



(a)

(b)

**Figure 3.5** The ionization chamber: a) FC65-P and b) CC13

### 3.6.4 Electrometer

The DOSE-1 is a high precision dosimeter reference class electrometer that significantly exceeds the recommendations of the IEC 60731 and the AAPM ADCLs. It is suitable for the use with ionization chambers, semiconductors and diamond probes. The standard DOSE-1 (Scanditronix, Wellhofer Dosimetries, Schwarzenbruck, Germany) connects to either TNC or BNC connector types. The reference voltage of this electrometer is +300 V. Maximum charge per pulse is approximate  $\pm 40$  nC/pulse. The DOSE-1 dosimeter is shown in figure 3.6.



**Figure 3.6** The DOSE-1 dosimeter

### 3.6.5 Eclipse treatment planning software

Eclipse treatment planning software version 8.9.17 (Varian Medical System, Palo Alto, CA, USA), which is shown in figure 3.7, is a treatment planning for all techniques such as conformal, IMRT and VMAT. The conventional technique is planned by forward planning, while IMRT and VMAT are planned by inverse planning using analytical anisotropic algorithm (AAA). The physicists and physicians used Eclipse treatment planning software to calculate the dose distribution and verify the best treatment plans for their patients.

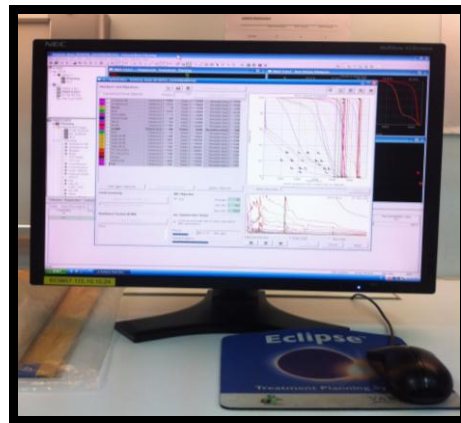
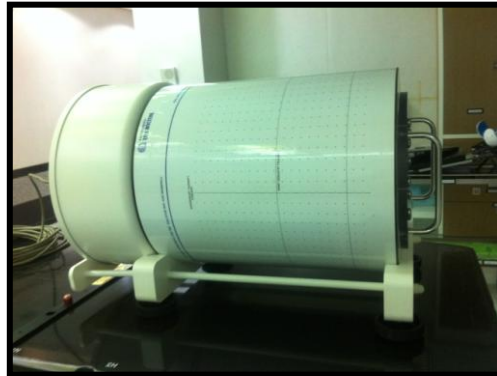


Figure 3.7 Eclipse treatment planning: version 8.9.17

### 3.6.6 Three-dimensional diode arrays: ArcCHECK [19]

Three-dimensional diode arrays: ArcCHECK™ (Sun Nuclear Corp., Melbourne, FL, USA) model 1220 is a cylindrical water-equivalent phantom with a three-dimensional array of 1386 diode detectors, arranged in a spiral pattern with 10 mm detector spacing. The inner section of acrylic phantom is 15 cm diameter. This phantom is possible to insert ionization chamber for patient point dose measurement. ArcCHECK is shown in figure 3.8.



**Figure 3.8** Three-dimensional diode arrays: ArcCHECK™

### **3.6.7 Solid water phantom**

The solid water phantom (RMI 457, CIVCO medical solution, IA, USA) made from epoxy resin based mixture which has the density (mass and electron density) of  $1.03 \text{ g/cm}^3$  and  $3.34 \times 10^{23} \text{ electron/g}$ , respectively. The solid water phantom has  $30 \times 30 \text{ cm}^2$  size with the thickness of 3 and 5 cm. The solid water phantoms are shown in figure 3.9.

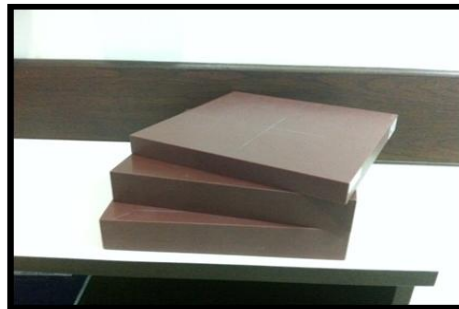


**Figure 3.9** Solid water phantoms

### **3.6.8 IMRT/VMAT QA software**

The SNC patient software (Sun Nuclear Corp., Melbourne, FL, USA) version 6.1 is software for IMRT/VMAT QA evaluation. The IMRT QA verification software is shown in figure 3.10. This software is used to compare two data sets of dose distribution (normally between planning calculation and ArcCHECK measurement).

The plan can be evaluated in absolute or relative, with gamma or only DTA analysis. It can be displayed in profile comparison across a selected axis. This software has a function of Calc Shift that can determine the misalignment between the planned and measured dose map and automatically corrects for the misalignment.

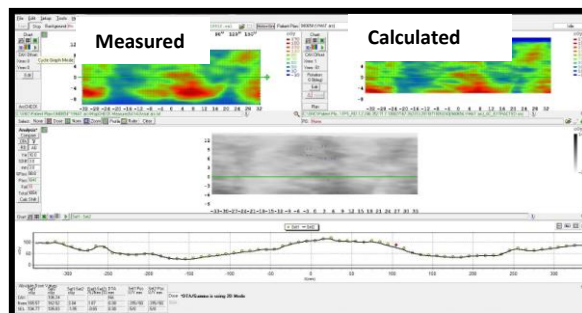


**Figure 3.10** SNC Patient software

### 3.7 Methods

The experiment is divided into 3 parts: gravitational effect of gantry, basic parameters and clinical applications.

#### 3.7.1 Basic parameters influenced the couches

##### 3.7.1.1 Gravitational effect of gantry rotation

The measurements were performed on Varian Clinac iX linear accelerator with 0.6 cc FC65-P ion chamber. The 1.5 cm and 2.5 cm diameter of buildup were inserted in the ion chamber which was placed in air at the isocenter to measure the gravitation effect of gantry rotation from  $0^\circ$  to  $360^\circ$  for 6 and 10 MV photon beams, respectively. The dose rate of 400 MU/min at  $10 \times 10 \text{ cm}^2$  field size, 100 cm SAD were acquired. The setup of FC65-P ion chamber is shown in figure 3.11.



**Figure 3.11** The chamber with buildup setting up on Varian Clinac iX linear accelerator

### 3.7.1.2 The Exact couch

Measurements were undertaken on linear accelerator, Clinac 21EX, which equips with Exact couch. The Exact couch has two sliding rails in and out position couch shown in figure 3.12 and a grid couch insert, all made of carbon fiber to support the patient. The cylindrical acrylic phantom was used to measure the dose in this study. The 0.65 cc Farmer type ion chamber which was positioned at the center of the cylindrical phantom was set to isocenter as shown in figure 3.13.

The phantom was aligned along the central axis of the gantry as defined by laser guide system. The gantry was rotated around the phantom from  $0^\circ$  to  $360^\circ$ , the measurement were undertaken for every 10 degrees.



(a)

(b)

**Figure 3.12** The Exact couch: a) sliding rail out and b) sliding rail in position



Then the average dose at beam angle of  $0^\circ$ ,  $90^\circ$ , and  $270^\circ$  will be employed as a normalized dose since there is no beam attenuation by the couch. The measurements were taken for both energy of 6 MV and 10 MV photon beams at field sizes of  $3 \times 3 \text{ cm}^2$ ,  $5 \times 5 \text{ cm}^2$ ,  $10 \times 10 \text{ cm}^2$ , and  $20 \times 20 \text{ cm}^2$ . The outputs of 100 MU and dose rate of 400 MU/min were employed. The Exact couch was studied in two longitudinal positions (cranial and caudal) for the sliding rails parked at “in” and “out” position.

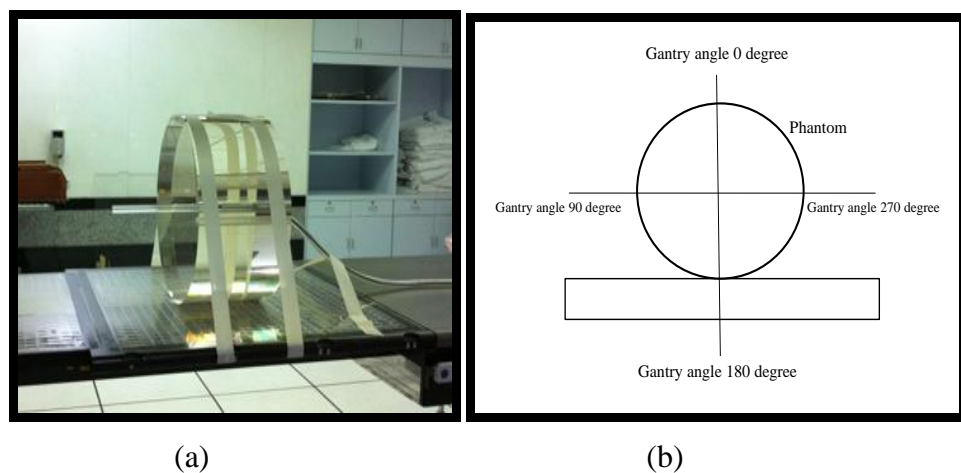


**Figure 3.13** a) The chamber and phantom setting up on Exact couch and b) diagram of gantry angle

### 3.7.1.3 The Exact IGRT couch

Measurements were performed on Varian linear accelerator, Clinac iX which equips with IGRT couch. The FC65-P ion chamber was inserted into the cylindrical acrylic phantom and the center of chamber was set at the isocenter as shown in figure 3.14. The phantom was positioned along the central axis of the gantry as defined by laser guided system.



**Figure 3.14** The chamber and phantom setting up on Exact IGRT couch

The measurements were undertaken from gantry angles of  $0^\circ$  to  $360^\circ$  then the average dose at beam angle of  $0^\circ$ ,  $90^\circ$ , and  $270^\circ$  were also used as a normalized dose. The measurements were taken for both energy of 6 MV and 10 MV photon beams at field sizes of  $3 \times 3 \text{ cm}^2$ ,  $5 \times 5 \text{ cm}^2$ ,  $10 \times 10 \text{ cm}^2$ , and  $20 \times 20 \text{ cm}^2$ . The outputs of 100 MU and dose rate of 400 MU/min were employed. The Exact IGRT couch was set at three longitudinal couch positions (cranial, middle and caudal).

### **3.7.2 Clinical application**

The second part for this study is to determine the effect of couch attenuation of conventional, IMRT, and VMAT treatment techniques. The patients were randomly selected from clinical database which all patients selected must be passed the criteria of having the posterior or posterior oblique fields.

#### **3.7.2.1 Conventional technique**

The patients planning in the Eclipse TPS database were chosen for the study. Patients were two brain, two lung, and two pelvis plans. The 6 MV doses for Exact couch with sliding rails park at “out” position for brain and lung cases were selected and 10 MV were used for pelvis cases. The three field plans of 0, 120 and 240 degree beams were employed.

The beam parameters of the patient plans were transferred to the square solid water phantom in treatment planning and the point doses were recalculated on the

phantom as a verification plan with the same patient beam parameters those are: energy, field size, dose, and dose rate. Then, the verification plans were exported to the treatment machine to measure the dose. FC65-P ionization chamber was inserted in the phantom at the isocenter of actual depth of the patient and the point measurement was compared with the calculation with and without couch insertion.

For sliding rail in of Exact couch and Exact IGRT couch, the patients of brain, lung and pelvis were planned with 2 fields arrangement at gantry angles of 0 and 180 degree. The collimator and couch rotation were set to 0 degrees without MLC for all plans. The spine plan was added for Exact IGRT couch. The measurements were undertaken for both without and with couch insertion.

#### 3.7.2.2 Intensity-modulated radiation therapy (IMRT)

For advance clinical application, the patients were scanned with CT-simulator and sent to treatment planning. Then the tumor and organs at risk were precisely delineated by the physician. The physicist optimized the plan with inverse treatment planning for IMRT and VMAT using concept of the objective function of the beamlet weights. The calculation was undertaken by consideration with couch and without couch insertion. The IMRT plans that were approved by physician were transferred to ArcCHECK device. The radiation doses were recalculated on ArcCHECK as a verification plan with the same patient beam parameter those are: energy, field size, dose, dose rate and MLC. Then, the verification plans were exported to the treatment machine to measure the dose. The ArcCHECK was placed on both treatment couches with 95.65 cm SSD setting up. The beams were set at the actual angles. The IMRT verifications with ArcCHECK were studied at rail “in” and “out” sliding rail position for exact couch and at cranial and caudal longitudinal position for Exact IGRT couch.

The comparison of calculated and measured dose was demonstrated by percent pass of gamma value: 3% dose difference and 3 mm distance to agreement. In addition, the point dose difference at the isocenter was reported.

#### 3.7.1.1.3 Volumetric-modulated arc therapy (VMAT)

The VMAT plans that were approved by physician were transferred to ArcCHECK device. The radiation doses were recalculated on ArcCHECK as a

verification plan with the same patient parameter those are: energy, field size, dose, dose rate, gantry speed, and MLC. Then, the verification plans were exported to the treatment machine to measure the dose. The VMAT verifications with ArcCHECK were studied at cranial for brain, middle for lung and caudal longitudinal position for pelvis in Exact IGRT couch.

The comparison of calculated and measured dose was demonstrated by percent pass of gamma value, 3% dose difference and 3 mm distance to agreement. In addition, the point dose difference at the isocenter was reported.

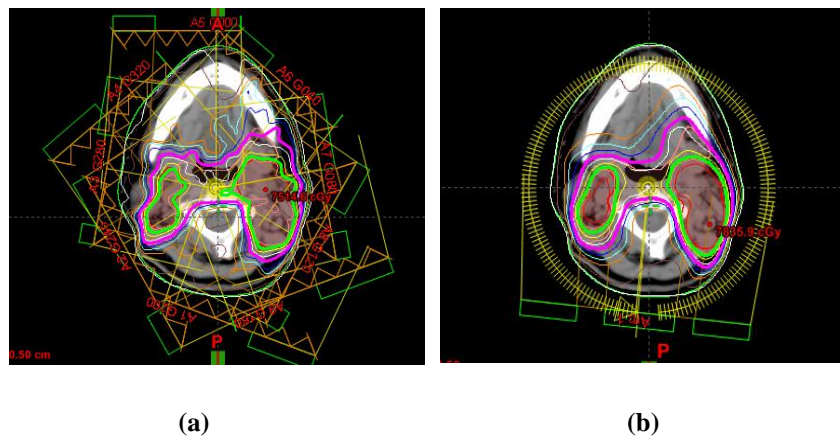


**Figure 3.15** Dose distributions of a) IMRT and b) VMAT techniques

### 3.8 Outcome Measurement

Independent variables are dose rate and treatment time.

Dependent variables are field size, energy, types of couch, couch position, beam angle and techniques.

### 3.9 Data Collection

After studying the basic dosimetric parameters influenced on the couch, the Exact couch and the IGRT couch were evaluated for conventional pretreatment verification in term of point dose difference, for IMRT and VMAT pretreatment

verification in term of the percent pass of gamma value. The percent pass and SD were record.

### **3.10 Data Analysis**

The gamma evaluation of 3% dose difference and 3 mm distance to agreement was used for the tolerance between measured and calculated dose.

### **3.11 Benefit of the Study**

1. The correct dose in the treatment of tumor will be attained.
2. The optimal parameters from treatment planning will be chosen to ensure that the QA results reflect the dose that patient actually receives. If possible, couch parameters or corrections will be included in treatment planning systems, and beam angles will be carefully selected to avoid patients underdose.

### **3.12 Ethical Consideration**

This study was performed on the phantom (not directly operate to the patient). However, the proposal was approved by the ethics committee of Faculty of Medicine, Chulalongkorn University.

## CHAPTER IV

### RESULTS

#### 4.1 Gravitational effect of gantry rotation

The gravitational effect on gantry was evaluated by repeated measuring the dose in air in every 20 degree from 0 to 360 degree for Varian Clinac iX. The collected signals were averaged for 2 times measurements and normalized to 0 degree gantry angle. The result which is shown in table 4.1 for 6 MV and table 4.2 for 10 MV demonstrated no gravitation effect when gantry was rotated.

**Table 4.1** Gravitational effect of gantry rotation at various angles for 6 MV and 10x10 cm<sup>2</sup> field size

Gantry angle (degree)	Collected signal		Ave. collected signal	Relative to 0 degree
	No. of measurement			
	1	2		
0	19.28	19.30	19.29	1.000
20	19.28	19.28	19.28	0.999
40	19.28	19.28	19.28	0.999
60	19.27	19.27	19.27	0.998
90	19.29	19.28	19.28	0.999
80	19.30	19.29	19.29	1.000
100	19.29	19.29	19.29	1.000
120	19.29	19.29	19.29	1.000
140	19.27	19.27	19.27	0.998
160	19.29	19.27	19.28	0.999
180	19.28	19.27	19.27	0.999
200	19.28	19.30	19.29	1.000
220	19.30	19.32	19.31	1.001
240	19.31	19.31	19.31	1.001
260	19.32	19.32	19.32	1.001
270	19.33	19.32	19.32	1.001
280	19.32	19.31	19.31	1.001
300	19.32	19.31	19.31	1.002
320	19.33	19.33	19.33	1.002
340	19.30	19.30	19.30	1.000
360	19.28	19.30	19.29	1.000

**Table 4.2** Gravitational effect of gantry rotation at various angles for 10 MV and 10x10 cm<sup>2</sup> field size

Gantry angle (degree)	Collected signal		Ave. collected signal	Relative to 0 degree
	No. of measurement			
	1	2		
0	10.71	10.72	10.72	1.000
20	10.72	10.72	10.72	1.000
40	10.71	10.72	10.72	1.000
60	10.73	10.72	10.73	1.001
90	10.74	10.73	10.74	1.002
80	10.74	10.74	10.74	1.002
100	10.74	10.73	10.74	1.002
120	10.73	10.73	10.73	1.001
140	10.74	10.73	10.73	1.001
160	10.72	10.73	10.73	1.001
180	10.71	10.71	10.71	0.999
200	10.71	10.71	10.71	0.999
220	10.71	10.71	10.71	0.999
240	10.71	10.70	10.70	0.998
260	10.71	10.71	10.71	0.999
270	10.70	10.70	10.70	0.998
280	10.71	10.73	10.71	0.999
300	10.71	10.71	10.71	0.999
320	10.71	10.72	10.72	1.000
340	10.72	10.72	10.72	1.000
360	10.71	10.72	10.72	1.000

Figure 4.1 a) and 4.1 b) are the polar plotted for gravitational effect of 0 to 360 degree gantry angle for 10x10 cm<sup>2</sup> field size. The circle dose illustrated that the doses around the isocenter were isotropic.

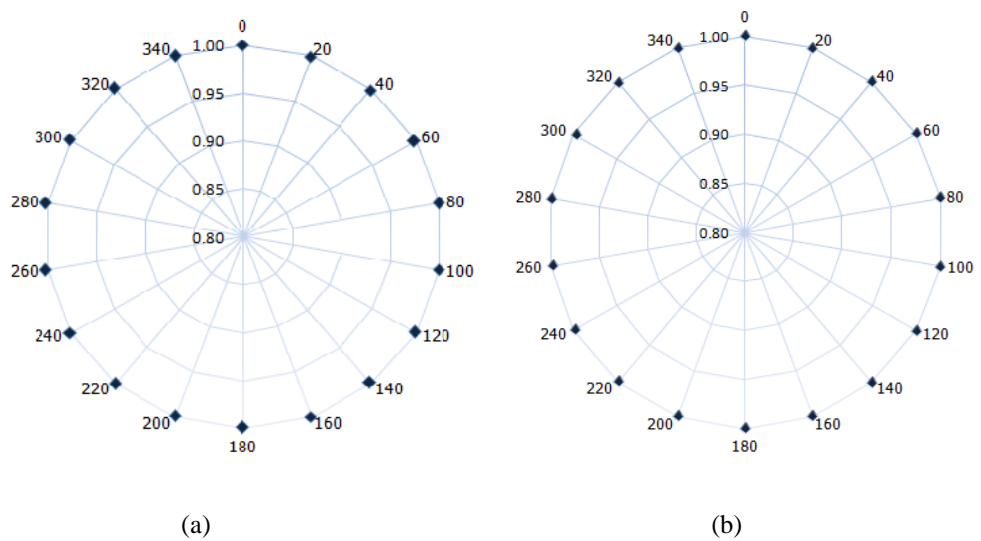


**Figure 4.1** The polar plot of relative dose for gravitation effect of gantry rotation for 10x10 cm<sup>2</sup> field size: a) 6 MV and b) 10 MV

## 4.2 Basic parameters influenced the Exact couch

### 4.2.1 Sliding rail out: *cranial position*

The results of transmitted dose from the Exact couch relative to average values of 0, 90, and 270 degree gantry angles from Clinac 21EX are shown in table 4.3 for 6 MV and table 4.4 for 10 MV with sliding rail out at cranial position for different field sizes from 3x3 to 20x20 cm<sup>2</sup>.



**Table 4.3** Relative doses from Exact couch for 6 MV with sliding rail out at *cranial position* for 3x3, 5x5, 10x10, and 20x20 cm<sup>2</sup> field sizes

Gantry angle (degree)	Field size (cm <sup>2</sup> )				Gantry angle (degree)	Field size (cm <sup>2</sup> )			
	3x3	5x5	10x10	20x20		3x3	5x5	10x10	20x20
0, 90, and 270	1.000	1.000	1.000	1.000	180	0.943	0.945	0.954	0.951
95	0.996	1.000	0.996	1.000	185	0.942	0.940	0.952	0.948
100	0.992	0.998	0.993	0.997	190	0.944	0.940	0.952	0.951
105	0.992	0.998	0.992	0.997	195	0.942	0.942	0.950	0.950
110	0.991	0.996	0.991	0.997	200	0.983	0.983	0.986	0.988
115	0.990	0.997	0.991	0.996	205	0.984	0.984	0.987	0.989
120	0.989	0.996	0.991	0.995	210	0.984	0.984	0.988	0.990
125	0.970	0.982	0.972	0.977	215	0.977	0.980	0.986	0.984
130	0.853	0.854	0.871	0.873	220	0.883	0.882	0.885	0.894
135	0.947	0.941	0.944	0.940	225	0.944	0.941	0.944	0.940
140	0.883	0.882	0.890	0.894	230	0.853	0.854	0.871	0.873
145	0.977	0.980	0.986	0.984	235	0.970	0.981	0.972	0.977
150	0.984	0.984	0.988	0.990	240	0.989	0.992	0.991	0.995
155	0.984	0.984	0.987	0.989	245	0.990	0.994	0.991	0.996
160	0.983	0.983	0.986	0.988	250	0.991	0.994	0.991	0.996
165	0.942	0.942	0.950	0.950	255	0.992	0.993	0.992	0.997
170	0.944	0.945	0.952	0.951	260	0.992	0.994	0.993	0.997
175	0.942	0.944	0.952	0.948	265	0.996	1.000	0.996	1.000

**Table 4.4** Relative doses from Exact couch for 10 MV with sliding rail out at *cranial position* for 3x3, 5x5, 10x10, and 20x20 cm<sup>2</sup> field sizes

Gantry angle (degree)	Field size (cm <sup>2</sup> )				Gantry angle (degree)	Field size (cm <sup>2</sup> )			
	3x3	5x5	10x10	20x20		3x3	5x5	10x10	20x20
0, 90, and 270	1.000	1.000	1.000	1.000	180	0.952	0.957	0.957	0.961
95	0.997	0.997	1.000	1.000	185	0.951	0.957	0.955	0.960
100	0.992	0.992	0.994	1.000	190	0.953	0.957	0.957	0.961
105	0.992	0.992	0.994	0.998	195	0.953	0.956	0.957	0.960
110	0.991	0.992	0.994	0.997	200	0.986	0.986	0.985	0.988
115	0.991	0.990	0.993	0.997	205	0.989	0.987	0.985	0.988
120	0.991	0.991	0.992	0.998	210	0.989	0.987	0.985	0.987
125	0.978	0.975	0.979	0.983	215	0.989	0.984	0.981	0.982
130	0.887	0.887	0.891	0.897	220	0.905	0.907	0.909	0.915
135	0.958	0.954	0.951	0.954	225	0.958	0.940	0.951	0.954
140	0.905	0.907	0.909	0.915	230	0.887	0.887	0.891	0.897
145	0.989	0.984	0.981	0.982	235	0.978	0.975	0.979	0.983
150	0.989	0.987	0.985	0.987	240	0.991	0.991	0.992	0.998
155	0.989	0.987	0.985	0.988	245	0.991	0.990	0.993	0.997
160	0.986	0.986	0.985	0.988	250	0.991	0.992	0.994	0.997
165	0.953	0.956	0.957	0.960	255	0.992	0.992	0.994	0.994
170	0.953	0.957	0.957	0.961	260	0.992	0.992	0.994	0.998
175	0.951	0.955	0.955	0.960	265	1.000	1.000	1.000	1.000

Figure 4.2 a) and 4.2 b) display the polar plot of relative dose for 6 MV and 10 MV photon beams, data from table 4.3 and 4.4, respectively. The relative transmitted doses for 120 to 240 degree counterclockwise illustrated almost isotopic, while the low doses were observed in: 130 to 140, 220 to 230, and 165 to 195 degree. The small field size showed more attenuation due to the couch than the larger field size and the low energy could more attenuate radiation than high energy. The maximum attenuation due to rail out was shown at 130 and 230 degree, 14.7% for 6 MV and 11.3% for 10 MV at 3x3 cm<sup>2</sup> field size, the attenuation in posterior part at 165 to 195 degree was 5.8% for 6 MV and 4.9% for 10 MV.

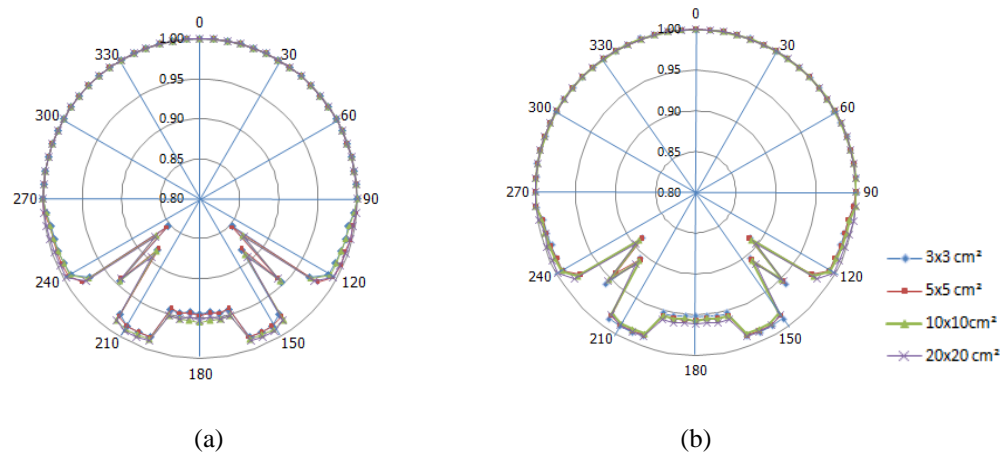


**Figure 4.2** The polar plot of relative dose for Exact couch with rail out position for 3x3, 5x5, 10x10, and 20x20 cm<sup>2</sup> field sizes: a) 6 MV and b) 10 MV

#### 4.2.2 Sliding rail in: *cranial position*

The results of response dose relative to average values of 0, 90, and 270 degree gantry angles are shown in table 4.5 for 6 MV and table 4.6 for 10 MV with sliding rail in position at cranial position for different field sizes from 3x3 to 20x20 cm<sup>2</sup>.

**Table 4.5** Relative doses from Exact couch for 6 MV with sliding rail in at *cranial position* for 3x3, 5x5, 10x10, and 20x20 cm<sup>2</sup> field sizes

Gantry angle (degree)	Field size (cm <sup>2</sup> )				Gantry angle (degree)	Field size (cm <sup>2</sup> )			
	3x3	5x5	10x10	20x20		3x3	5x5	10x10	20x20
0 ,90, and 270	1.000	1.000	1.000	1.000	180	0.942	0.944	0.943	0.946
95	0.995	0.995	0.996	1.000	185	0.817	0.821	0.835	0.850
100	0.990	0.991	0.993	0.997	190	0.815	0.820	0.831	0.844
105	0.990	0.991	0.993	0.997	195	0.841	0.846	0.852	0.867
110	0.989	0.991	0.992	0.997	200	0.968	0.967	0.967	0.972
115	0.988	0.990	0.992	0.997	205	0.983	0.983	0.981	0.985
120	0.988	0.989	0.991	0.996	210	0.984	0.982	0.983	0.986
125	0.981	0.983	0.991	0.988	215	0.983	0.981	0.982	0.985
130	0.979	0.980	0.981	0.985	220	0.983	0.984	0.984	0.987
135	0.981	0.982	0.984	0.986	225	0.981	0.982	0.984	0.986
140	0.983	0.984	0.984	0.987	230	0.979	0.980	0.981	0.985
145	0.983	0.981	0.982	0.985	235	0.981	0.983	0.991	0.988
150	0.984	0.982	0.983	0.986	240	0.988	0.989	0.991	0.996
155	0.983	0.983	0.981	0.985	245	0.988	0.990	0.992	0.997
160	0.968	0.967	0.967	0.972	250	0.989	0.991	0.992	0.997
165	0.841	0.846	0.852	0.867	255	0.990	0.991	0.993	0.997
170	0.815	0.820	0.831	0.844	260	0.990	0.991	0.993	0.997
175	0.817	0.821	0.835	0.850	265	0.995	0.995	0.996	1.000

**Table 4.6** Relative doses from Exact couch for 10 MV with sliding rail in at *cranial position* for 3x3, 5x5, 10x10, and 20x20 cm<sup>2</sup> field sizes

Gantry angle (degree)	Field size (cm <sup>2</sup> )				Gantry angle (degree)	Field size (cm <sup>2</sup> )			
	3x3	5x5	10x10	20x20		3x3	5x5	10x10	20x20
0, 90, and 270	1.000	1.000	1.000	1.000	180	0.953	0.955	0.958	0.963
95	0.997	0.997	1.000	1.000	185	0.853	0.861	0.872	0.882
100	0.994	0.995	0.996	0.999	190	0.854	0.859	0.868	0.877
105	0.994	0.994	0.995	0.998	195	0.871	0.877	0.886	0.893
110	0.992	0.994	0.994	0.997	200	0.974	0.973	0.976	0.978
115	0.992	0.994	0.994	0.996	205	0.984	0.986	0.988	0.990
120	0.991	0.993	0.994	0.996	210	0.987	0.986	0.988	0.988
125	0.985	0.986	0.987	0.990	215	0.989	0.985	0.986	0.988
130	0.983	0.985	0.985	0.989	220	0.987	0.988	0.988	0.989
135	0.985	0.987	0.986	0.989	225	0.985	0.987	0.986	0.989
140	0.987	0.988	0.988	0.989	230	0.983	0.985	0.985	0.989
145	0.989	0.985	0.986	0.988	235	0.985	0.986	0.987	0.990
150	0.987	0.986	0.988	0.988	240	0.991	0.993	0.994	0.996
155	0.984	0.986	0.988	0.990	245	0.992	0.994	0.994	0.996
160	0.974	0.973	0.976	0.978	250	0.992	0.994	0.994	0.997
165	0.871	0.877	0.886	0.893	255	0.994	0.994	0.995	0.998
170	0.853	0.859	0.868	0.877	260	0.994	0.995	0.996	0.999
175	0.854	0.861	0.872	0.882	265	0.997	0.997	1.000	1.000

Figure 4.3 a) and 4.3 b) display the polar plot of relative doses for 6 MV and 10 MV photon beams, data from table 4.5 and 4.6, respectively. The relative doses for 160 to 200 degree counterclockwise illustrated almost isotopic, while the low doses were observed in: 165 to 175, and 185 to 195 degree. The small field size also showed more attenuation due to the couch than the larger field size and the low energy could more attenuate radiation than high energy. The maximum attenuation was shown at 170 and 190 degree, 18.5% for 6 MV and 14.7% for 10 MV in 3x3 cm<sup>2</sup> field size.

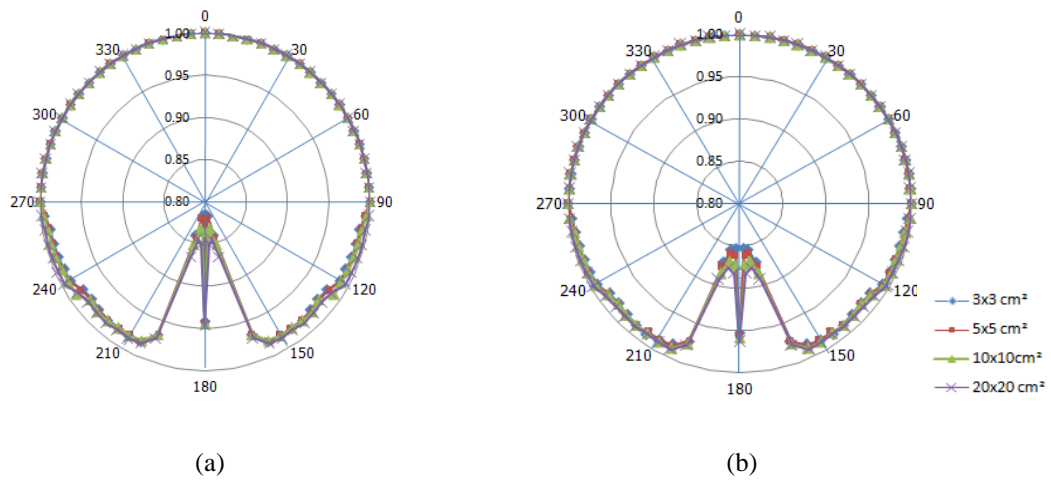


**Figure 4.3** The polar plot of relative dose for Exact couch with rail in position for 3x3, 5x5, 10x10, and 20x20 cm<sup>2</sup> field sizes: a) 6 MV and b) 10 MV

#### 4.2.3 Sliding rail out: *caudal position*

The results of response dose relative to average values of 0, 90, and 270 degree gantry angle are shown in table 4.7 for 6 MV and table 4.8 for 10 MV at sliding rail out position with caudal position for different field sizes from 3x3 to 20x20 cm<sup>2</sup>.

**Table 4.7** Relative doses from Exact couch for 6 MV with sliding rail out at *caudal position* for 3x3, 5x5, 10x10, and 20x20 cm<sup>2</sup> field sizes

Gantry angle (degree)	Field size (cm <sup>2</sup> )				Gantry angle (degree)	Field size (cm <sup>2</sup> )			
	3x3	5x5	10x10	20x20		3x3	5x5	10x10	20x20
0, 90, and 270	1.000	1.000	1.000	1.000	180	1.000	0.997	0.997	0.997
95	0.999	1.000	0.999	1.000	185	0.997	0.997	0.996	0.997
100	0.999	0.999	0.999	0.999	190	0.993	0.997	0.995	0.997
105	0.997	0.997	0.999	0.999	195	0.993	0.997	0.995	0.997
110	0.995	0.995	0.999	0.999	200	0.990	0.996	0.995	0.997
115	0.995	0.995	0.995	0.995	205	0.990	0.996	0.995	0.997
120	0.994	0.994	0.991	0.992	210	0.990	0.995	0.996	0.996
125	0.873	0.879	0.884	0.894	215	0.991	0.990	0.988	0.989
130	0.873	0.879	0.884	0.894	220	0.868	0.875	0.883	0.893
135	0.949	0.952	0.949	0.952	225	0.949	0.952	0.949	0.952
140	0.868	0.875	0.883	0.893	230	0.873	0.879	0.884	0.894
145	0.991	0.990	0.988	0.989	235	0.873	0.879	0.884	0.894
150	0.990	0.995	0.996	0.996	240	0.994	0.994	0.991	0.992
155	0.990	0.996	0.995	0.997	245	0.995	0.995	0.995	0.995
160	0.990	0.996	0.995	0.997	250	0.995	0.995	0.999	0.999
165	0.993	0.997	0.995	0.997	255	0.997	0.997	0.999	0.999
170	0.993	0.997	0.995	0.997	260	0.996	0.995	0.996	0.997
175	0.997	0.997	0.996	0.997	265	0.999	1.000	0.999	1.000

**Table 4.8** Relative doses from Exact couch for 10 MV with sliding rail out at *caudal position* for 3x3, 5x5, 10x10, and 20x20 cm<sup>2</sup> field sizes

Gantry angle (degree)	Field size (cm <sup>2</sup> )				Gantry angle (degree)	Field size (cm <sup>2</sup> )			
	3x3	5x5	10x10	20x20		3x3	5x5	10x10	20x20
0, 90, and 270	1.000	1.000	1.000	1.000	180	1.000	0.996	0.996	0.998
95	0.997	0.997	0.998	1.000	185	1.000	0.995	0.996	0.998
100	0.996	0.996	0.998	0.999	190	0.998	0.993	0.995	0.997
105	0.996	0.996	0.998	0.999	195	0.997	0.993	0.995	0.997
110	0.996	0.996	0.998	0.999	200	0.996	0.993	0.995	0.997
115	0.994	0.994	0.996	0.997	205	0.996	0.993	0.995	0.997
120	0.993	0.993	0.994	0.995	210	0.996	0.993	0.995	0.997
125	0.907	0.910	0.916	0.921	215	0.993	0.990	0.990	0.993
130	0.901	0.905	0.907	0.918	220	0.898	0.900	0.907	0.914
135	0.960	0.960	0.962	0.965	225	0.960	0.960	0.962	0.965
140	0.898	0.900	0.907	0.914	230	0.901	0.905	0.907	0.918
145	0.993	0.990	0.990	0.993	235	0.907	0.910	0.916	0.921
150	0.996	0.993	0.995	0.997	240	0.993	0.993	0.994	0.995
155	0.996	0.993	0.995	0.997	245	0.994	0.994	0.996	0.997
160	0.996	0.993	0.995	0.997	250	0.996	0.996	0.998	0.999
165	0.997	0.993	0.995	0.997	255	0.996	0.996	0.998	0.999
170	0.998	0.993	0.995	0.997	260	0.996	0.996	0.998	0.999
175	1.000	0.995	0.996	0.998	265	0.997	0.997	0.998	1.000

Figure 4.4 a) and 4.4 b) display the polar plot of relative dose for 6 MV and 10 MV photon beams, data from table 4.7 and 4.8, respectively. The same pattern of attenuation as the cranial was obtained but the lower effect detected due to no center plate supported in caudal position. The relative doses for 120 to 240 degree counterclockwise illustrated almost isotopic, while the low doses were observed in: 125 to 140, and 220 to 235 degree. The small field size showed more attenuation due to the couch than the larger field size and the low energy could more attenuate radiation than high energy. The maximum attenuation was shown at 140 and 220 degree, 13.2% for 6 MV and 10.2% for 10 MV at 3x3 cm<sup>2</sup> field size.



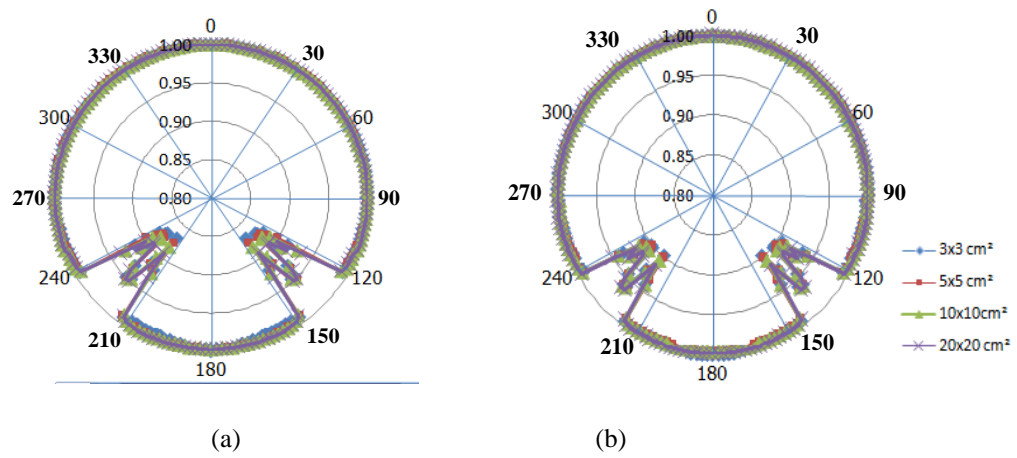


**Figure 4.4** The polar plot of relative dose for Exact couch with rail out position for 3x3, 5x5, 10x10, and 20x20 cm<sup>2</sup> field sizes: a) 6 MV and b) 10 MV

#### 4.2.4 Sliding rail in: *caudal position*

The results of response dose relative to 0, 90, and 270 degree gantry angle are shown in table 4.9 for 6 MV and table 4.10 for 10 MV with sliding rail in position at caudal position for different field size from 3x3 to 20x20 cm<sup>2</sup>.

**Table 4.9** Relative doses from Exact couch for 6 MV with sliding rail in at *caudal position* for 3x3, 5x5, 10x10, and 20x20 cm<sup>2</sup> field sizes

Gantry angle (degree)	Field size (cm <sup>2</sup> )				Gantry angle (degree)	Field size (cm <sup>2</sup> )			
	3x3	5x5	10x10	20x20		3x3	5x5	10x10	20x20
0, 90, and 270	1.000	1.000	1.000	1.000	180	0.985	0.992	0.988	0.991
95	0.997	0.996	0.997	0.997	185	0.848	0.858	0.870	0.884
100	0.996	0.995	0.996	0.997	190	0.857	0.864	0.874	0.886
105	0.996	0.996	0.996	0.997	195	0.872	0.883	0.891	0.902
110	0.996	0.996	0.996	0.997	200	0.948	0.945	0.948	0.955
115	0.992	0.994	0.992	0.993	205	0.991	0.991	0.991	0.993
120	0.988	0.992	0.988	0.989	210	0.991	0.9900	0.991	0.994
125	0.987	0.991	0.987	0.989	215	0.991	0.990	0.991	0.993
130	0.987	0.989	0.987	0.988	220	0.991	0.989	0.991	0.992
135	0.991	0.989	0.991	0.992	225	0.991	0.989	0.991	0.992
140	0.991	0.989	0.991	0.992	230	0.987	0.989	0.987	0.988
145	0.991	0.990	0.991	0.993	235	0.987	0.991	0.987	0.989
150	0.991	0.9900	0.991	0.994	240	0.988	0.992	0.988	0.989
155	0.991	0.991	0.991	0.993	245	0.992	0.994	0.992	0.993
160	0.948	0.945	0.948	0.955	250	0.996	0.996	0.996	0.997
165	0.872	0.883	0.891	0.902	255	0.996	0.996	0.996	0.997
170	0.857	0.864	0.874	0.886	260	0.996	0.995	0.996	0.997
175	0.848	0.858	0.870	0.884	265	0.997	0.996	0.997	0.997

**Table 4.10** Relative doses from Exact couch for 10 MV with sliding rail in at *caudal position* for 3x3, 5x5, 10x10, and 20x20 cm<sup>2</sup> field sizes

Gantry angle (degree)	Field size (cm <sup>2</sup> )				Gantry angle (degree)	Field size (cm <sup>2</sup> )			
	3x3	5x5	10x10	20x20		3x3	5x5	10x10	20x20
0, 90, and 270	1.000	1.000	1.000	1.000	180	0.988	0.995	0.994	0.998
95	0.999	0.999	0.999	0.998	185	0.882	0.894	0.899	0.908
100	0.999	0.999	0.998	0.998	190	0.888	0.898	0.902	0.911
105	0.999	0.999	0.998	0.998	195	0.901	0.911	0.916	0.922
110	0.999	0.999	0.998	0.999	200	0.951	0.962	0.965	0.965
115	0.997	0.997	0.998	0.996	205	0.995	0.995	0.995	0.996
120	0.996	0.996	0.998	0.993	210	0.995	0.995	0.995	0.996
125	0.995	0.995	0.996	0.993	215	0.995	0.995	0.994	0.996
130	0.994	0.994	0.994	0.993	220	0.994	0.994	0.993	0.995
135	0.994	0.994	0.994	0.994	225	0.994	0.994	0.994	0.994
140	0.994	0.994	0.993	0.995	230	0.994	0.994	0.994	0.993
145	0.995	0.995	0.994	0.996	235	0.995	0.995	0.996	0.993
150	0.995	0.995	0.995	0.996	240	0.996	0.996	0.998	0.993
155	0.995	0.995	0.995	0.996	245	0.997	0.997	0.998	0.996
160	0.951	0.962	0.965	0.965	250	0.999	0.999	0.998	0.999
165	0.901	0.911	0.916	0.922	255	0.999	0.999	0.998	0.998
170	0.888	0.898	0.902	0.911	260	0.999	0.999	0.998	0.998
175	0.882	0.894	0.899	0.908	265	0.999	0.999	0.999	0.998

Figure 4.5 a) and 4.5 b) display the polar plot of relative dose for 6 MV and 10 MV photon beams, data from table 4.9 and 4.10, respectively. The same pattern of attenuation as the cranial was obtained but the lower effect detected due to no center plate supported in caudal position. The relative doses for 160 to 200 degree counter-clockwise illustrated almost isotopic, while the low doses were observed in: 165 and 175, and 185 to 195 degree. The small field size showed more attenuation due to the couch than the larger field size and the low energy could more attenuate radiation than high energy. The maximum attenuation was shown at 175 and 185 degree, 15.2% for 6 MV and 11.8% for 10 MV at 3x3 cm<sup>2</sup> field size.

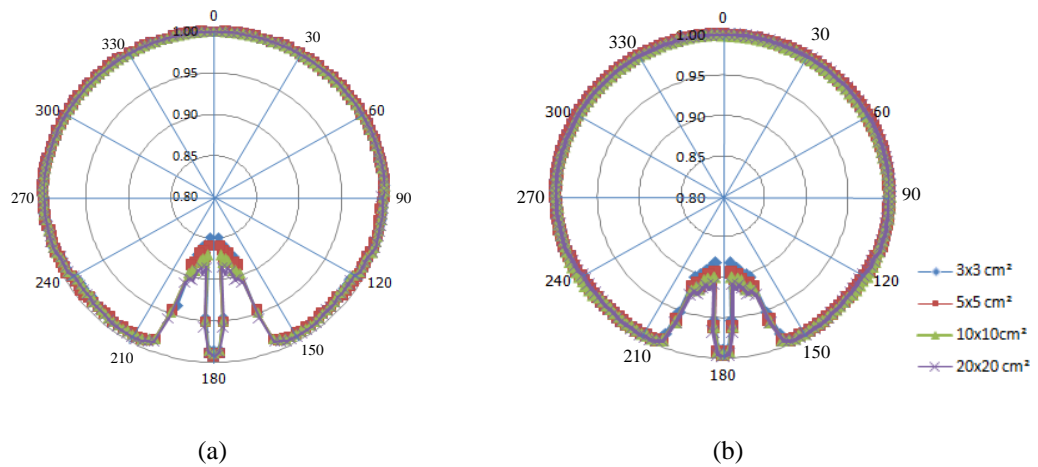


**Figure 4.5** The polar plot of relative dose for Exact couch with rail in position for 3x3, 5x5, 10x10, and 20x20 cm<sup>2</sup> field sizes: a) 6 MV and b) 10 MV

#### 4.2.5 Summary of field size effect for the Exact couch

Table 4.11 shows maximum attenuation introduced by couch with sliding rails in and out at cranial position of the Exact couch for different field sizes. The attenuation effect was pronounced in small field size and high energy. The attenuation was more in rail in than rail out position. The maximum attenuation of 6 MV with sliding rail in and rail out ranged from 15.6% to 18.5% and 12.7% to 14.7%, respectively, for field size of 20x20 cm<sup>2</sup> down to 3x3 cm<sup>2</sup>. The maximum attenuation of 10 MV with sliding rail in and out ranged from 12.2% to 14.7% and 10.3% to 11.3%, respectively, for field size of 20x20 cm<sup>2</sup> down to 3x3 cm<sup>2</sup>.

Table 4.12 shows maximum attenuation introduced by couch with sliding rail in and out at caudal position. The maximum attenuation of 6 MV with sliding rail in and rail out ranged from 11.6% to 15.2% and 10.7% to 13.2%, respectively, for field size of 20x20 cm<sup>2</sup> down to 3x3cm<sup>2</sup>. The maximum attenuation of 10MV with sliding rail in and out ranged from 9.2% to 11.8% and 8.6% to 10.2%, respectively, for field size of 20x20 cm<sup>2</sup> down to 3x3 cm<sup>2</sup>. The cranial position showed more attenuation than the caudal.

**Table 4.11** Maximum attenuation introduced by couch (with sliding rails out and in at cranial position for the Exact couch)

Energy	Position of sliding rail	Gantry angle (degree)	Field size (cm <sup>2</sup> )			
			3x3	5x5	10x10	20x20
6 MV	Out	130	14.7%	14.6%	12.9%	12.7%
10 MV	Out	130	11.3%	11.3%	10.9%	10.3%
6 MV	In	170	18.5%	18.0%	16.9%	15.6%
10 MV	In	170	14.7%	14.1%	13.2%	12.2%

**Table 4.12** Maximum attenuation introduced by couch (with sliding rails out and in at caudal position for the Exact couch)

Energy	Position of sliding rail	Gantry angle (degree)	Field size (cm <sup>2</sup> )			
			3x3	5x5	10x10	20x20
6 MV	Out	140	13.2%	12.5%	11.7%	10.7%
10 MV	Out	140	10.2%	10.0%	9.3%	8.6%
6 MV	In	175	15.2%	14.2%	13.0%	11.6%
10 MV	In	175	11.8%	10.6%	10.1%	9.2%

### 4.3 Basic parameters influenced the Exact IGRT couch

#### 4.3.1 Cranial position

The results of response dose relative to average values of 0, 90, and 270 degree gantry angles are shown in table 4.13 for 6 MV and table 4.14 for 10 MV at cranial position for different field sizes from 3x3 to 20x20 cm<sup>2</sup>.

**Table 4.13** Relative doses from Exact IGRT couch for 6 MV at *cranial position* for 3x3, 5x5, 10x10, and 20x20 cm<sup>2</sup> field sizes

Gantry angle (degree)	Field size (cm <sup>2</sup> )				Gantry angle (degree)	Field size (cm <sup>2</sup> )			
	3x3	5x5	10x10	20x20		3x3	5x5	10x10	20x20
0, 90, and 270	1.000	1.000	1.000	1.000	180	0.976	0.975	0.977	0.977
100	0.997	1.000	0.997	1.000	190	0.975	0.974	0.976	0.978
110	0.999	1.000	0.998	1.000	200	0.973	0.973	0.976	0.977
120	0.996	0.999	0.996	1.000	210	0.971	0.971	0.973	0.976
130	0.966	0.968	0.969	0.973	220	0.967	0.968	0.970	0.973
140	0.967	0.968	0.970	0.973	230	0.966	0.968	0.969	0.973
150	0.971	0.971	0.973	0.976	240	0.996	0.999	0.996	1.000
160	0.973	0.973	0.976	0.977	250	0.999	1.000	0.998	1.000
170	0.975	0.974	0.976	0.978	260	0.997	1.000	0.997	1.000

**Table 4.14** Relative doses from Exact IGRT couch for 10 MV at *cranial position* for 3x3, 5x5, 10x10, and 20x20 cm<sup>2</sup> field sizes

Gantry angle (degree)	Field size (cm <sup>2</sup> )				Gantry angle (degree)	Field size (cm <sup>2</sup> )			
	3x3	5x5	10x10	20x20		3x3	5x5	10x10	20x20
0, 90, and 270	1.000	1.000	1.000	1.000	180	0.989	0.981	0.987	0.984
100	1.000	1.000	1.000	0.999	190	0.986	0.979	0.986	0.982
110	1.000	1.000	1.000	0.998	200	0.984	0.979	0.985	0.981
120	1.000	1.000	1.000	0.997	210	0.982	0.979	0.983	0.979
130	0.981	0.976	0.980	0.977	220	0.980	0.976	0.981	0.977
140	0.980	0.976	0.981	0.977	230	0.981	0.976	0.980	0.977
150	0.982	0.979	0.983	0.979	240	1.000	1.000	1.000	0.997
160	0.984	0.979	0.985	0.981	250	1.000	1.000	1.000	0.998
170	0.986	0.979	0.986	0.982	260	1.000	1.000	1.000	0.999

Figure 4.6 a) and 4.6 b) display the polar plot of relative dose for 6 MV and 10 MV photon beams, data from table 4.13 and 4.14, respectively. The relative doses for 120 to 240 degree counterclockwise illustrated almost isotopic. The rest angle showed less attenuation and also lesser than Exact couch. The small field size also showed more attenuation due to the couch than the larger field size and the low energy could attenuate radiation than high energy. The maximum attenuation was shown at 140 and 220 degree, 3.3% for 6 MV and 2.0% for 10 MV at 3x3 cm<sup>2</sup> field size.

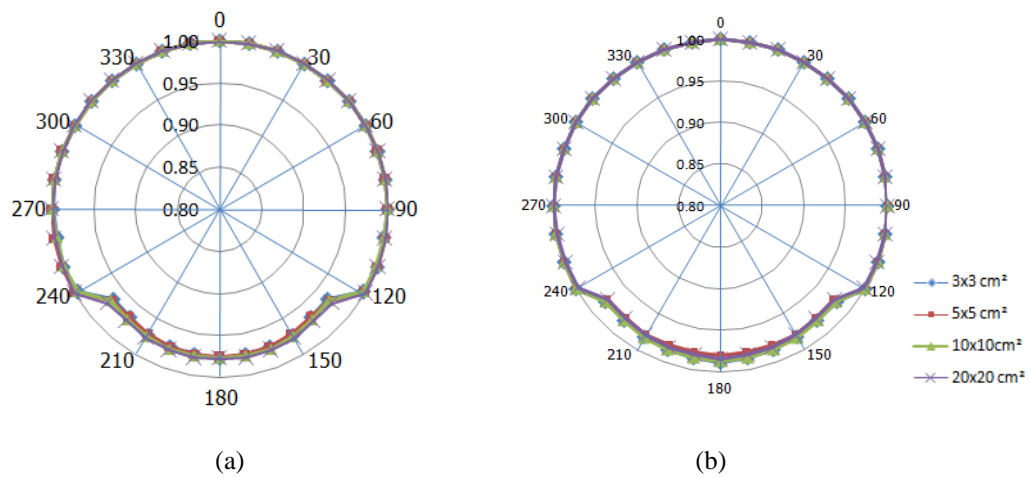


**Figure 4.6** The polar plot of relative dose at cranial position for the Exact IGRT couch for 3x3, 5x5, 10x10, and 20x20 cm<sup>2</sup> field sizes: a) 6 MV and b) 10 MV

### 4.3.2 Middle position

The results of response dose relative to average values of 0, 90, and 270 degree gantry angles are shown in table 4.15 for 6 MV and table 4.16 for 10 MV at middle position for different field sizes from 3x3 to 20x20 cm<sup>2</sup>.

**Table 4.15** Relative doses from Exact IGRT couch for 6 MV at *middle position* for 3x3, 5x5, 10x10, and 20x20 cm<sup>2</sup> field sizes

Gantry angle (degree)	Field size (cm <sup>2</sup> )				Gantry angle (degree)	Field size (cm <sup>2</sup> )			
	3x3	5x5	10x10	20x20		3x3	5x5	10x10	20x20
0, 90, and 270	1.000	1.000	1.000	1.000	180	0.973	0.970	0.973	0.976
100	1.000	1.000	1.000	1.000	190	0.970	0.969	0.971	0.974
110	1.000	1.000	0.999	1.000	200	0.969	0.969	0.970	0.973
120	1.000	0.997	0.996	0.997	210	0.968	0.965	0.967	0.970
130	0.968	0.965	0.967	0.970	220	0.965	0.963	0.966	0.968
140	0.965	0.963	0.966	0.968	230	0.968	0.965	0.967	0.970
150	0.968	0.965	0.967	0.970	240	1.000	0.997	0.996	0.997
160	0.969	0.969	0.970	0.973	250	1.000	1.000	0.999	1.000
170	0.970	0.969	0.971	0.974	260	1.000	1.000	1.000	1.000

**Table 4.16** Relative doses from Exact IGRT couch for 10 MV at *middle position* for 3x3, 5x5, 10x10, and 20x20 cm<sup>2</sup> field sizes

Gantry angle (degree)	Field size (cm <sup>2</sup> )				Gantry angle (degree)	Field size (cm <sup>2</sup> )			
	3x3	5x5	10x10	20x20		3x3	5x5	10x10	20x20
0, 90, and 270	1.000	1.000	1.000	1.000	180	0.974	0.980	0.980	0.983
100	0.999	1.000	1.000	1.000	190	0.971	0.979	0.979	0.983
110	0.992	1.000	1.000	1.000	200	0.969	0.977	0.978	0.982
120	0.992	1.000	0.999	1.000	210	0.965	0.975	0.977	0.980
130	0.967	0.975	0.976	0.979	220	0.967	0.974	0.974	0.978
140	0.965	0.974	0.974	0.978	230	0.967	0.975	0.976	0.979
150	0.967	0.975	0.977	0.980	240	0.992	1.000	0.999	1.000
160	0.969	0.977	0.978	0.982	250	0.997	1.000	1.000	1.000
170	0.971	0.979	0.979	0.983	260	0.998	1.000	1.000	1.000

Figure 4.7 a) and 4.7 b) display the polar plot of relative dose for 6 MV and 10 MV photon beams, data from table 4.15 and 4.16, respectively. The relative doses for 120 to 240 degree counterclockwise illustrated almost isotopic. The rest showed less attenuation and also lesser than Exact couch. The small field size also showed more attenuation due to the couch than the larger field size and the low energy could attenuate radiation than high energy. The maximum attenuation was shown at 140 and 220 degree, 3.5% for both 6 MV and 10 MV at 3x3 cm<sup>2</sup> field size.

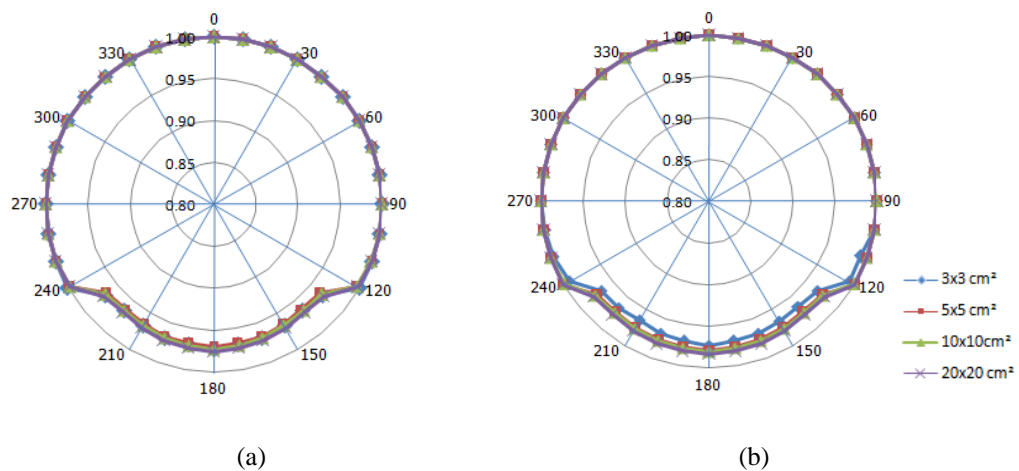


**Figure 4.7** The polar plot of relative dose at middle position for the Exact IGRT couch for 3x3, 5x5, 10x10, and 20x20 cm<sup>2</sup> field sizes: a) 6 MV and b) 10 MV



### 4.2.3 Caudal position

The results of response dose relative to average values of 0, 90, and 270 degree gantry angles are shown in table 4.17 for 6 MV and table 4.18 for 10 MV on caudal position at different field sizes from 3x3 to 20x20 cm<sup>2</sup>.

**Table 4.17** Relative doses from Exact IGRT couch for 6 MV at *caudal position* for 3x3, 5x5, 10x10, and 20x20 cm<sup>2</sup> field sizes

Gantry angle (degree)	Field size (cm <sup>2</sup> )				Gantry angle (degree)	Field size (cm <sup>2</sup> )			
	3x3	5x5	10x10	20x20		3x3	5x5	10x10	20x20
0, 90, and 270	1.000	1.000	1.000	1.000	180	0.952	0.956	0.961	0.965
100	0.999	0.994	0.995	0.994	190	0.950	0.954	0.958	0.962
110	0.996	0.994	0.993	0.994	200	0.949	0.953	0.957	0.960
120	0.994	0.993	0.991	0.990	210	0.949	0.951	0.955	0.958
130	0.955	0.955	0.956	0.958	220	0.949	0.950	0.954	0.956
140	0.949	0.951	0.954	0.956	230	0.955	0.956	0.956	0.958
150	0.949	0.951	0.955	0.958	240	0.994	0.993	0.991	0.990
160	0.949	0.953	0.957	0.960	250	0.996	0.994	0.993	0.994
170	0.950	0.954	0.958	0.962	260	0.999	0.994	0.995	0.994

**Table 4.18** Relative doses from Exact IGRT couch for 10 MV at *caudal position* for 3x3, 5x5, 10x10, and 20x20 cm<sup>2</sup> field sizes

Gantry angle (degree)	Field size (cm <sup>2</sup> )				Gantry angle (degree)	Field size (cm <sup>2</sup> )			
	3x3	5x5	10x10	20x20		3x3	5x5	10x10	20x20
0, 90, and 270	1.000	1.000	1.000	1.000	180	0.950	0.971	0.974	0.978
100	1.000	1.000	0.997	0.996	190	0.950	0.969	0.972	0.976
110	1.000	0.994	0.992	1.000	200	0.950	0.968	0.971	0.976
120	0.999	0.994	0.992	1.000	210	0.964	0.965	0.969	0.975
130	0.969	0.967	0.968	0.977	220	0.965	0.964	0.967	0.974
140	0.965	0.964	0.967	0.974	230	0.969	0.967	0.968	0.977
150	0.964	0.965	0.969	0.975	240	0.999	0.994	0.992	1.000
160	0.950	0.968	0.971	0.976	250	1.000	0.994	0.992	1.000
170	0.950	0.969	0.972	0.976	260	1.000	0.997	0.996	1.000

Figure 4.8 a) and 4.8 b) display the polar plot of relative dose for 6 MV and 10 MV photon beams, data from table 4.17 and 4.18, respectively. The relative doses for 120 to 240 degree counterclockwise illustrated almost isotropic. The rest showed less attenuation and also lesser than Exact couch. The small field size also showed more attenuation due to the couch than the larger field size and the low energy could attenuate radiation than high energy. The maximum attenuation was shown at 140 and 220 degree for both 6 MV and 10 MV for all field sizes except 10 MV at 3x3 cm<sup>2</sup> field size. The maximum was shown at 5.1% for 6 MV and 5.0% for 10 MV at 3x3 cm<sup>2</sup> field size.

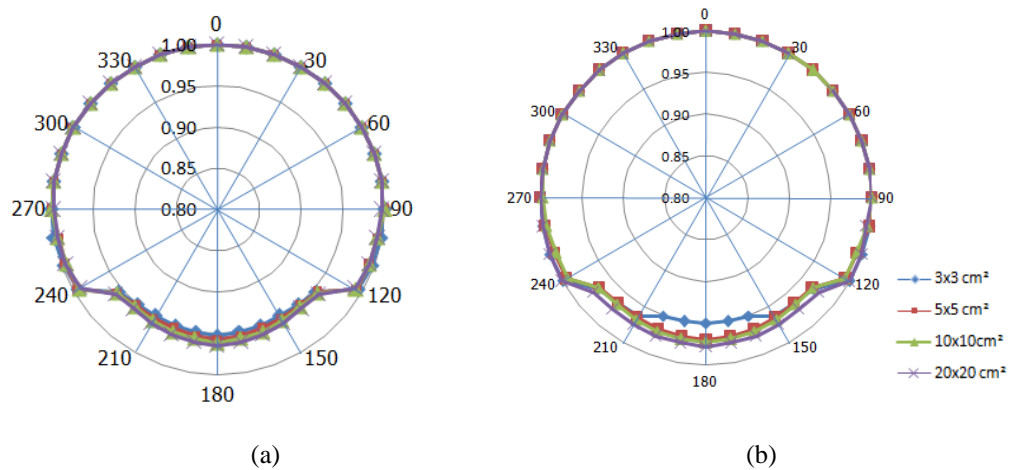


**Figure 4.8** The polar plot of relative dose at caudal position for the Exact IGRT couch for 3x3, 5x5, 10x10, and 20x20 cm<sup>2</sup> field sizes: a) 6 MV and b) 10 MV

#### 4.3.4 Summary of field size effect for the Exact IGRT couch

Table 4.19 shows the maximum attenuation introduced by couch at cranial, middle and caudal position of the Exact couch for different field sizes. The attenuation was more in caudal than cranial and middle position. The maximum attenuation of 6 MV was up to 5.1%, 4.9%, 4.6%, and 4.4%, for field size of 3x3 cm<sup>2</sup>, 5x5 cm<sup>2</sup>, 10x10 cm<sup>2</sup>, and 20x20 cm<sup>2</sup>, respectively. The maximum attenuation of 10 MV was 5.1%, 3.6%, 3.3%, and 2.6% at 3x3 cm<sup>2</sup>, 5x5 cm<sup>2</sup>, 10x10 cm<sup>2</sup>, and 20x20 cm<sup>2</sup>, respectively.

**Table 4.19** The maximum attenuation introduced by couch at cranial, middle and caudal position for *the Exact IGRT couch*

Energy	Field size (cm <sup>2</sup> )			
	3x3	5x5	10x10	20x20
Cranial Position				
6 MV	3.3%	3.2%	3.0%	2.7%
10 MV	2.8%	2.6%	2.5%	2.2%
Middle position				
6 MV	3.5%	3.7%	3.4%	3.2%
10 MV	3.5%	2.6%	2.6%	2.2%
Caudal position				
6 MV	5.1%	4.9%	4.6%	4.4%
10 MV	5.0%	3.6%	3.3%	2.6%

#### 4.4 Clinical application

##### 4.4.1 Conventional technique

In clinical part of patient treatment, the isocenter dose was measured in solid water phantom. Table 4.20 shows the isocenter dose comparison between measurement and planning without and with Exact couch inserted for sliding rail out. The 3 field plans of 0, 120 and 240 degree beam were employed for brain, lung and pelvis. The differences between planning with couch and measurement were 0.62%, 0.31% and 0.42% for brain (6 MV), lung (6 MV), and pelvis (10 MV), respectively. The differences between planning without couch and measurement were 0.82%, 2.05% and 0.83% for brain (6 MV), lung (6 MV), and pelvis (10 MV), respectively. The differences were more in planning without couch.

**Table 4.20** Dose difference between calculation and measurement with the sliding rail “out” position of conventional techniques for *the Exact couch*

Region	Planning with couch (cGy)	Planning without couch (cGy)	Measurement (cGy)	Dose difference between measurement and planning	
				With couch	Without couch
Brain (6 MV: 3 fields)	207.60	210.50	208.78	0.62%	0.82%
Lung (6 MV: 3 fields)	195.30	200.00	195.90	0.31%	2.05%
Pelvis (10 MV: 3 fields)	205.00	207.60	205.87	0.42%	0.83%

Table 4.21 shows the dose comparison between measurement and planning with and without Exact couch inserted with sliding rail in. The parallel field plans of 0 and 180 degree beam were employed for brain, lung and pelvis. The differences between planning with couch and measurement were 0.14%, 0.34% and 2.08% for brain (6 MV), lung (6 MV), and pelvis (10 MV), respectively. The differences between planning without couch and measurement were 5.99%, 7.96% and 4.84% for brain (6 MV), lung (6 MV), and pelvis (10 MV), respectively. The differences were more in planning without couch. The sliding rail in were more different than sliding rail out.

**Table 4.21** Dose difference between calculation and measurement with the sliding rail “in” position of conventional techniques for *the Exact couch*

Region	Planning with couch (cGy)	Planning without couch (cGy)	Measurement (cGy)	Dose difference between planning and measurement	
				With couch	Without couch
Brain (6 MV: 2 fields)	198.30	210.50	198.59	0.14%	5.99%
Lung (6 MV: 2 fields)	177.80	191.30	177.18	0.34%	7.96%
Pelvis (10 MV: 2 fields)	191.30	200.00	195.38	2.08%	4.84%

Table 4.22 shows the dose comparison between measurement with and without Exact IGRT couch inserted. The parallel field plans of 0 and 180 degree beam were employed for brain, lung and pelvis at cranial, middle and caudal couch position, respectively. The dose difference between measurement with couch and without couch were 1.51%, 0.79%, 1.04%, and 2.29% for brain (6 MV), lung (6 MV), pelvis (10 MV), and spine (6 MV) plan, respectively. The attenuation effect was less in Exact IGRT couch than Exact couch.

**Table 4.22** Dose difference between measurement with and without couch of conventional technique for *the Exact IGRT couch*

Region	Measurement with couch (cGy)	Measurement without couch (cGy)	Dose difference between measurement with and without couch
1. Brain (6 MV: 2 fields)	94.94	96.40	1.51%
2. Lung (6 MV: 2 fields)	209.90	211.58	0.79%
3. Pelvis (10 MV: 2 fields)	204.52	206.68	1.04%
4. Spine (6 MV: 1 field)	215.27	220.32	2.29%

#### 4.4.2 Intensity-modulated radiation therapy (IMRT)

The ArcCHECK measurement doses with Exact couch inserted were compared with the treatment planning calculation with and without couch of different region with the % pass criteria of gamma index of 3%, 3mm. For 9 plans of brain, lung in cranial and pelvis in caudal with rail out couch position (3 plans in each region), we found that the % gamma pass of all clinical case studies with couch insertion were higher than without couch and % point dose difference also showed better result for both types of couch. The maximum % dose difference at isocenter was 5.89% at brain region for the Exact couch, and 3.25% at pelvis for the Exact IGRT couch. The results of IMRT technique for the Exact couch and the Exact IGRT couch are shown in table 4.23 and table 4.24, respectively.

**Table 4.23** The percent gamma pass and percent dose difference between measurements compared to planning with and without couch insertion for IMRT techniques for *the Exact couch*

Region	% gamma pass ( $\pm$ SD)		% dose difference ( $\pm$ SD)	
	With couch	Without couch	With couch	Without couch
Brain (6 MV: 5/7 fields)**	95.30%( $\pm$ 2.68)	89.80%( $\pm$ 9.19)	1.51%( $\pm$ 1.26)	5.89%( $\pm$ 2.63)
Lung (6MV: 4/7 fields)*	98.00%( $\pm$ 0.91)	95.83%( $\pm$ 0.76)	2.31%( $\pm$ 1.04)	3.50%( $\pm$ 0.66)
Pelvis (10 MV: 4/7 fields)*	97.90%( $\pm$ 1.04)	96.29%( $\pm$ 0.45)	1.60%( $\pm$ 1.45)	2.67%( $\pm$ 2.00)

**Table 4.24** The percent gamma pass and percent dose difference between measurements compared to planning with and without couch insertion for IMRT technique for *the Exact IGRT couch*

Region	% gamma pass ( $\pm$ SD)		% dose difference ( $\pm$ SD)	
	With couch	Without couch	With couch	Without couch
Brain (6 MV: 4/7 fields)*	99.13%( $\pm$ 1.15)	97.56%( $\pm$ 0.75)	0.26%( $\pm$ 0.19)	0.67%( $\pm$ 0.26)
Lung (6 MV: 4/7 fields)*	98.90%( $\pm$ 1.07)	96.23%( $\pm$ 1.05)	2.11%( $\pm$ 0.74)	2.83%( $\pm$ 0.77)
Pelvis (10 MV: 5/9 fields)***	99.26%( $\pm$ 1.27)	98.00%( $\pm$ 1.73)	2.54%( $\pm$ 1.24)	3.25%( $\pm$ 0.42)

\* (4/7 fields) means 4 from 7 fields pass through the couch.

\*\* (5/7 fields) means 5 from 7 fields pass through the couch

\*\*\* (5/9 fields) means 5 from 9 fields pass through the couch.

#### 4.4.3 Volumetric-modulated arc therapy (VMAT)

The clinical cases were examined for 3 regions at different positions of Exact IGRT couch: brain in cranial, lung in middle and pelvis in caudal couch positions. The % gamma pass compared between measurement and calculation with couch insertion was slightly higher than without couch and % point dose difference also showed better result. The dose difference without couch ranged from 2.87 to 4.73% and with couch ranged from 0.79 to 4.22%.

**Table 4.25** The percent gamma pass and percent dose difference between measurement compared to planning with and without couch insertion of the VMAT technique for *the Exact IGRT couch*

Region	% gamma pass ( $\pm$ SD)		% dose difference ( $\pm$ SD)	
	With couch	Without couch	With couch	Without couch
Brain	97.20%( $\pm$ 0.77)	95.60%( $\pm$ 0.98)	2.22%( $\pm$ 0.13)	3.97%( $\pm$ 1.19)
Lung	98.30%( $\pm$ 0.21)	98.10%( $\pm$ 0.28)	4.22%( $\pm$ 0.39)	4.73%( $\pm$ 0.14)
Pelvis	98.70%( $\pm$ 0.49)	98.50%( $\pm$ 1.62)	0.79%( $\pm$ 0.45)	2.87%( $\pm$ 0.04)

## CHAPTER V

### DISCUSSION AND CONCLUSIONS

#### 5.1 Discussion

##### 5.1.1 Gravitation effect of gantry rotation

The responses of gravitation effect of gantry angle varying from 0 to 360 degree show the circle dose with the largest deviation of only  $\pm 0.2\%$ . The circle doses illustrate that the doses around the isocenter are isotropic. There is no effect of gravitation.

##### 5.1.2 Basic parameters influence the Exact couch

The Exact couch attenuation effects depend on field size, energy, beam angle, couch longitudinal position and sliding rail position.

For the field size, the maximum couch attenuation in 6 MV beams is 18.5% for 3x3 cm<sup>2</sup> field size for Exact couch at sliding rail in that agreed with Li et al. who reported 16.0% attenuation for 6 MV with 3x3 cm<sup>2</sup>. The dose error due to the effect of couch attenuation increase when the small field sizes are used. The smaller field has more beam attenuation than larger field because the smaller field lacks of side scatter electronic equilibrium. The influences of field size are observed in the sliding rail in, rail out and both couch position (cranial and caudal).

The attenuation of 6 MV photon beams is higher than that of 10 MV beams. The high energy is more penetrate through the couch, so the lower energy presents more couch attenuation effect. The attenuation of 18.5% is observed in 6 MV with sliding rail in cranial position, compared with 14.7% for 10 MV, with the same parameters.

The couch attenuation is also strongly angular dependence, which is relied on the couch design, especially in the angle of beam passing through the thicker part of the couch. The suitable beam direction should be selected to avoid the rail position. The maximum relative dose is shown in the gantry angle ranged from 170 and 190



degree: 18.5% for 6 MV and 14.7% for 10 MV at 3x3 cm<sup>2</sup> field size. The results were comparable with Li et al who reported 16.0% for 6 MV at 3x3 cm<sup>2</sup> field size of maximum attenuation at the gantry angle ranged from 150 to 210 degree.

The position of longitudinal couch demonstrates the different values of couch attenuation due to the construction of couch longitudinal position designed. The maximum attenuation up to 18.5% and 15.2% are observed in 6 MV with cranial and caudal position, respectively. The results agreed with Vieira et al. who presented the maximum attenuation in H&N region (cranial position) of 15.0%. The Exact couch attenuation effect is more introduced in cranial (brain and chest cases) than caudal position (pelvis case) because couch at pelvis part has only carbon fiber tennis racket but the upper part has a thick carbon fiber plate part at the central of couch.

The sliding rail in position is more attenuated than rail out. The maximum attenuation of 6 MV with sliding rail in and rail out were 18.5% and 14.7%, respectively. The sliding rail in makes the beam pass through the rail thickness and include more beam attenuation from the center plate supported, while the beams from sliding rail out does not pass through it.

### **5.1.3 Basic parameters influence the Exact IGRT couch**

The Exact IGRT couch attenuation effect also depends on field size, energy, beam angle and couch longitudinal position.

For the field size, the maximum couch attenuation for 6 MV beams range from 3.2 to 4.9% for 5x5 cm<sup>2</sup> field size and from 3.0% to 4.6% for 10x10 cm<sup>2</sup> field size. The results agree with Li et al. who showed the range from 3.8% to 4.8% for 5x5 cm<sup>2</sup> field size and from 2.9% to 4.1% for 10x10 cm<sup>2</sup> field size, and also confirmed with Vanetti et al. who reported 3.1% to 4.4% for 10x10 cm<sup>2</sup> in 6 MV. The effect of couch attenuation is smaller than the Exact couch. The Exact IGRT couch makes from the homogeneous air equivalent while the Exact couch consists of air equivalent material and metal rail support. So the attenuation effect is more in Exact couch.

The attenuation of 6 MV photon beams is higher than that of 10 MV beams. The high energy is more penetrated through the couch, so the lower energy presents more couch attenuation effect. The attenuation of 4.9% is observed in 6 MV in caudal position, compared with 3.5% for 10 MV for 5x5 cm<sup>2</sup> in the same parameters that agree with Li et al. who reported 4.8% for 6 MV with 5x5 cm<sup>2</sup>.

The couch attenuation is also strongly angular dependence, which is relied on the couch design. The maximum reduction of relative dose is shown in the gantry angle ranged from 140 to 220 degree: 5.1% for 6 MV and 5.0% for 10 MV at 3x3 cm<sup>2</sup> field size. The results are comparable with Li et al. who reported 4.8% of maximum attenuation at the gantry angle ranged from 150 to 210 degree.

The couch longitudinal position has different thickness of carbon fiber designed for suitable supported in different regions. The maximum attenuation for 6 MV with cranial, middle and caudal position are 3.3%, 3.7% and 5.1%, respectively. The Exact couch attenuation effects are more introduced in caudal position (pelvis case) and middle (chest cases) than cranial (brain cases) because couch at caudal part has the maximum thickness.

Although the Varian treatment couch makes from carbon fiber, the couch attenuation effect is still presented in both Exact and Exact IGRT couches. The effect of Exact couch is more than the Exact IGRT Couch. The couch attenuation effect depends on field size, energy and couch position.

#### **5.1.4 Clinical application**

The dose for conventional plan between measurement and planning without and with Exact couch inserted with sliding rail out are less difference than sliding rail in. The maximum difference occurred in lung case for parallel opposing fields; they are 7.96% (without couch) and 0.34% (with couch) with sliding rail in position.

For the Exact IGRT couch, the dose difference between measurement with and without couch is highest to 2.29% in spine case, while the brain, lung and pelvis cases

illustrated small difference of less than 1.5% because this group employs 2 fields with one posterior field passed through the couch. In spine case, only one beam is passing through the couch. The beams pass through the couch 100% for spine case, while it is only 50% for the other plans.

In IMRT plan, the difference of the measured to the calculated point doses are more for without couch insertion than with couch insertion in both couch types, the maximum deviation between without couch and with Exact couch insertion is observed in brain case, 5.89% and 1.51%, respectively. The ArcCHECK results show slightly higher of percent gamma pass of 3% dose difference and 3 mm distance-to-agreement criteria with 10% threshold when comparing with the calculation of couch insertion than without couch insertion.

In VMAT techniques that employ only the Exact IGRT couch, the dose error effect of couch attenuation mostly increase than IMRT techniques using both couch types. The percent gamma pass with couch is slightly higher than without couch. When the TPS without couch inserted are considered, the dose differences range from 2.87% to 4.73% and with couch range from 0.79% to 4.22%.

## **5.2 CONCLUSIONS**

The impact of the dose differences due to couch attenuation of two types of Varian couch depend on field size, energy, beam angle, couch and sliding rail position. The dose effect from beam attenuation by the treatment couch is significant for patients treated with posterior or oblique posterior field, particularly those patients treated with small single field and low energy beam. The planner should avoid the beam directly pass through the posterior and posterior oblique (especially directly pass though the rail position in Exact couch) or the correction should be included in treatment planning systems. The Exact IGRT couch is a choice for all types of radiation treatment techniques due to less effect of attenuation than Exact couch.

### **5.3 RECOMMENDATION**

1. The change of doses near the surface due to the couch insertion should be studied to determine the occurrence of skin reaction.

2. The suitable CT number to correct for the couch attenuation in treatment planning should be studied.

## References

- [1] Faiz, M.K. The physics of radiation therapy. Third edition. Philadelphia PA USA: Lippincott William and Wilkins, 2003.
- [2] Internal Commission on Radiation Units and Measurements. The quality factor in radiation protection. ICRU Report No. 40, Michigan, 1986.
- [3] Bucci, M.K., Bevan, A., and Roach, M. Advances in Radiation Therapy: conventional to 3D, to IMRT, to 4D, and Beyond. CA Cancer J Clin 55 (March 2005): 114-134.
- [4] Johns, H.E. The physics of radiology. Second edition. New York, 1966.
- [5] EVANS, M.D.C. Radiation Oncology Physics. Quebec Canada: McGill University Health Center, 2006.
- [6] William, P. Review of Radiation Oncology Physics: A Handbook for Teachers and Students. (May 1, 2003). Austria, 2003.
- [7] Radiological Society of North America (RSNA) and American College of Radiology (ACR). Intensity modulated radiotherapy (IMRT) [Online]. 2008. Available from:  
<http://www.radiologyinfo.org/en/info.cfm?pg=imrt>
- [8] IOP Publishing. Volumetric modulated radiotherapy (VMAT) [Online].2009. Availablefrom:<http://medicalphysicsweb.org/cws/article/opinion/39542>
- [9] United States Food and Drug Administration, Overview of Device Regulation (2009).[http://www.varian.com/us/oncology/treatments/treatment\\_techniques/IMRT/benefits.html](http://www.varian.com/us/oncology/treatments/treatment_techniques/IMRT/benefits.html).
- [10] Sue, E., and Chris, A. Radiotherapy: Principles to Practice. First edition. New York, 1994.

- [11] Tom, D.A. quantitative evaluation of IMRT dose distributions: refinement and clinical assessment of the gamma evaluation. Radiotherapy and Oncology 62 (2002): 309-319.
- [12] Van Dyk, J., Barnett, R.B., Cygler, J.E., and Shragge, P.C. Commissioning and quality assurance of treatment planning computers. Int J Radiat Oncol Biol Phys 26 (May 1993): 261-273.
- [13] Low, D.A., Harms, W.B., Mutic, S., and Purdy, J.A. A technique for the quantitative evaluation of dose distributions. Med Phys 25 (May 1998): 656-661.
- [14] Heng, L., Andrew, K.L., and Jennifer, L.J. Characterization of dose impact on IMRT and VMAT from couch attenuation for two Varian couches. J Appl Clin Med Phys 12, 3 (2011): 23-31.
- [15] Vieira, S.C., Kaatee, R.S., Dirkx, M.L., and Heijmen, B.J. Two-dimensional measurement of photon beam attenuation by the treatment couch and immobilization devices using an electronic portal imaging device. Med Phys. (2003): 81- 87.
- [16] Jan, K.H.S., and Jarmo, A.J.K. Increased beam attenuation and surface dose by different couch inserts of treatment tables in megavoltage radiotherapy. J Appl Clin Med Phys 12, 4 (2011): 14-23.
- [17] Zhihui, H., Jianrong, D., and Liang, L. Evaluating and modeling of photon beam attenuation by a standard treatment couch. J Appl Clin Med Phys 12, 4 (2011): 139-146.
- [18] FC65P ionization chamber user's guide. Scanditronix Wellhofer, 2001.
- [19] ArcCHECK<sup>TM</sup> user's guide. The ultimate 4D QA solution. Sun Nuclear Corporation.

## Vitae

Name	<b>Narumol Nguanthean</b>
Date of Birth	April 17, 1978
Place of Birth	Nakhon Sawan, Thailand
Institution Attended	Faculty of Medical Technology, Ramkhumhang University
Present Address	127/2 No.516 Fatluacha, Payathai, Thailand. 10400